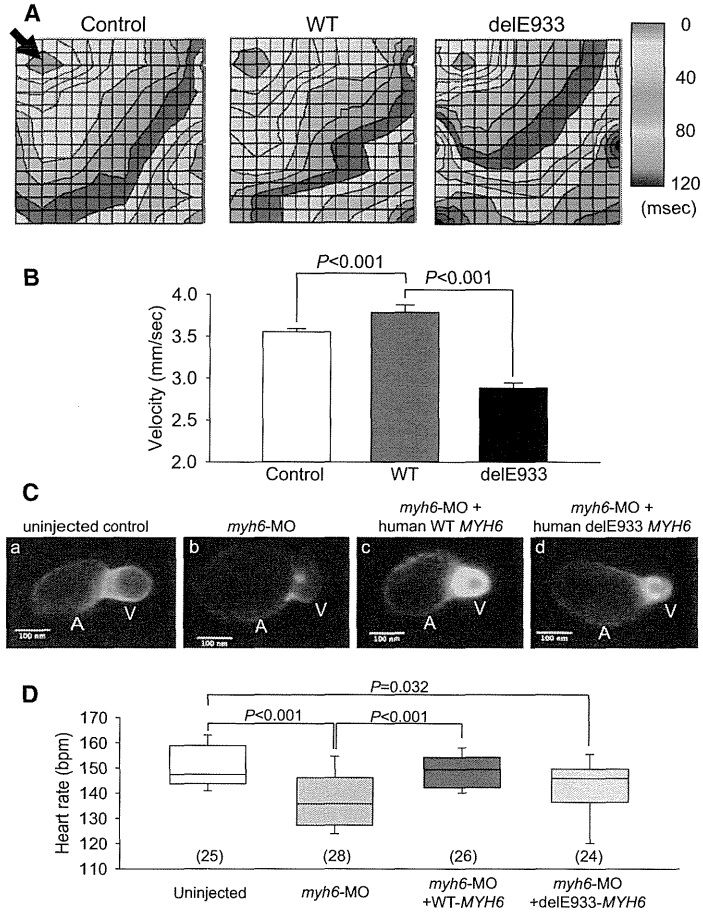

Figure 4. Electrophysiological phenotypes of delE933-*MYH6*. **A**, Representative activation isochronal maps of HL-1 cells stably expressing wild-type (WT) or delE933 *MYH6* and control HL-1 cells. An electric provocation with 10 μA was input on the pointed electrode (arrow). **B**, Averaged conduction velocity calculated from the time elapsed for the impulse to reach all remaining electrodes (n=252 for each recording). **C**, Representative fluorescent diastolic images of embryonic zebrafish hearts (atrium [A], ventricle [V]) at 48 hpf: uninjected control (**a**), *myh6*-MO only (**b**), *myh6*-MO coinjected with human WT *MYH6* cRNA (**c**), and *myh6*-MO coinjected with human delE933 *MYH6* cRNA (**d**). The atria of the *myh6* MO morphant in the presence or absence of coinjected human *MYH6* cRNAs (**b-d**) were slightly dilated compared with the uninjected control (**a**). The ventricle and cardiac looping pattern of the morphants, with or without *MYH6* cRNAs, were similar to that of the control. Scale bars, 100 μm **D**, Heart rate recordings from zebrafish (**a–d**). Data are shown as box and whisker plots with minimum, maximum, median, 25th, and 75th quartiles bars. Number in parentheses represents the number of zebrafish in each group.

Discussion

A growing body of evidence from genome-wide association studies has demonstrated an association of *MYH6* with sinus node function.[17–20] A common nonsynonymous single-nucleotide polymorphism of *MYH6* (A1101V) was previously shown to be a genetic modifier for resting heart rate and PR interval,[18] and this was further replicated in a large meta-analysis, including subjects of European ancestry from both the United States and Europe.[17,19] A combination of A1101V with other loci controlling heart rate further reduced the risk of SSS and pacemaker implantation, implicating a heritable quantitative trait.[17] By contrast, the rare *MYH6* variation R721W, unique to Icelanders, predisposes individuals to SSS and pacemaker implantation.[20] These studies clearly demonstrate that *MYH6* is a genetic modifier of sinus node function, but the mechanisms of this have been unclear, and it was uncertain whether *MYH6* could be a causative gene of familial SSS.

In this study, we identified a novel *MYH6* mutation, delE933, in one SSS individual among 9 probands of our familial SSS cohort.[22] We found that the mutant delE933-*MYH6* slowed down action potential propagation when heterologously expressed in the atrial myocardial cell line HL-1 (Figure 4A). Moreover, knockdown of endogenous *MYH6* leading to reduced heart rate in zebrafish could be compensated for by the coexpression of WT-*MYH6* but not by delE933-*MYH6* (Figure 4B). To our knowledge, this is the first experimental evidence demonstrating that *MYH6* variations can influence heart rate and action potential propagation. However, limited information is available to delineate the functional link between sarcomere components and sinus node function, and it remains unknown whether α-MHC directly affects pacemaker function or whether its actions are mediated though undefined mechanisms.

The delE933 mutation is located in the coiled-coil structure of the α-MHC S2 region, a binding motif for MyBP-C, and so is predicted to alter the tertiary structure and the cross-linking affinity between 2 sarcomere components (Figure 2A and 2B). Although the final consequences of such structural and functional modifications are unknown, a previous study that the MyBP-C mutation E334K, responsible for hypertrophic cardiomyopathy, impaired the ubiquitin-proteasome system, leading to an accumulation of cardiac ion channels at the sarcomere and electrophysiological dysfunction.[32] Increased protein levels were also observed for several other cardiac ion channels, including Kv1.5, Nav1.5, HCN4, Cav3.2, Cav1.2, SERCA, RYR2, and NCX1, which play major roles in controlling normal pacemaker function and atrial conductivity. Based on these findings, we speculate that an abnormal association

between delE933-α-MHC and MyBP-C might modulate the expression of cardiac ion channels that affect pacemaker function, which in turn would lead to the development of SSS.

In the present study, overexpression of the SSS-susceptible α-MHC mutants of R721W and delE933 in neonatal rat ventricular cardiomyocytes impaired sarcomere structures. However, it is unknown whether *MYH6* mutations preferentially impair the sinus node function or whether they might eventually cause further extensive electric damage manifesting as atrial fibrillation. Because the patient did not undergo electrophysiological studies or cardiac biopsy, further information regarding the spatial distribution and heterogeneity of pathological damages and electrophysiological abnormalities in the atrium is not available. Nevertheless, the T wave inversion of ECG and mild dilatation of the right atrium and LV (Figure 1A and 1B) are in accordance with the observation that targeted *myh6* knockdown in zebrafish induced the atrial dilatation associated with negative chronotropic effects, indicating that *MYH6* mutations may directly cause substantial damage and electric disorder to the myocardium in the atrium. This idea is further supported by the finding that heterozygous zebrafish expressing the *MYH6* mutation N695K (*MYH6*$^{hu/423/+}$) exhibited loss of atrial contractility, with residual beating restricted to the region near the atrioventricular junction and sinus venosus.[21] These observations strongly suggest that the final consequences of *MYH6* mutations in humans might also exhibit considerable heterogeneity with respect to the structural and electrophysiological properties of the atrium and sinus node.[33,34] Furthermore, these structural abnormalities of atrial sarcomere may extend to more severe conduction dysfunctions, such as atrial fibrillation or contractile failure, depending on the functional severity caused by each mutation. The slower conduction velocity observed in the HL-1 cells stably expressing delE933-*MYH6* in the present study suggests the possible involvement of *MYH6* in conduction dysfunction. This idea is supported by a recent genome-wide association study in which correlation studies of the *MYH6* variant R721W exhibited a significantly higher association with atrial fibrillation both before (odds ratio, 2.39; P=0.00010) and after (odds ratio, 2.03; P=0.015) exclusion of known SSS cases.[20] It is of note that the R719W of the ventricular β-MHC gene *MYH7*, homologous to the R721W-*MYH6*, is responsible for a malignant hypertrophic cardiomyopathy frequently associated with conduction abnormalities,[35] suggesting that α-MHC and β-MHC may share some pathophysiological mechanisms affecting cardiac action potential propagation.

SSS commonly occurs in older individual in the absence of accompanying heart diseases but comprises a variety of electrophysiological abnormalities in sinus node impulse formation and propagation. Although less common, SSS also shows familial inheritance, and implicated causative genes include those encoding cardiac ion channels, such as *SCN5A*. We recently found that familial SSS probands carrying *SCN5A* mutations showed a significantly earlier disease onset and a strong male predominance, whereas nonfamilial SSS had a disease onset of over 70 years for both sexes, which were affected equally.[22] The affected members of the SSS family in the present study were both women, aged over 60 years, suggesting that familial SSS with *MYH6* mutations might constitute an SSS subgroup distinct from that caused by *SCN5A* mutations. This may suggest the existence of a new disease entity of inherited arrhythmias attributable to mutations in genes encoding sarcomere proteins other than cardiac ion channel or ion channel-associated genes.

Limitation of the Study

Lack of information about the genotype–phenotype cosegregation of delE933-*MYH6* is the major limitation of this study from the standpoint of human genetics. Although bioinformatics evaluations, as well as in vitro and in vivo studies, have suggested pathophysiological significance of the rare *MYH6* variation delE933, it still does not exclude the possibility that the proband manifested SSS attributable to factors, such as aging rather than the *MYH6* mutation. To demonstrate the causality between SSS and *MYH6*, more extensive genetic screenings in patients with familial SSS to find novel *MYH6* mutations are required. Furthermore, it remains to be elucidated how the impaired sarcomere structures and conduction velocity elicited by delE933-*MYH6* ultimately result in the sinus node dysfunction. Electrophysiological studies using induced pluripotent stem cell–derived cardiomyocytes from *MYH6* mutation carriers, as well as basic evaluations of *MYH6* using genetically engineered animals, are also warranted.

Acknowledgments

We are indebted to Saori Nakano, Atsuko Iida, and Yasuko Noguchi for technical assistance and attending physicians for referring SSS patients.

Sources of Funding

This work was supported by Grant-in-Aid for Scientific Research on Innovative Areas (HD Physiology) 22136007 (N. Makita) and Grants-in-Aid for Scientific Research 26860572 (T. Ishikawa), 24390199 (N. Makita), 25293181 and 25670172 (A. Kimura) from the Ministry of Education, Culture, Sports, Science and Technology, Japan; Research Grant for the Cardiovascular Diseases (H24-033) from the Japanese Ministry of Health, Labour and Welfare (N. Makita); the Joint Usage/Research Program of Medical Research Institute Tokyo Medical and Dental University (N. Makita, A.K.); a research grant from Fukuda Foundation for Medical Technology (T. Ishikawa); Joint Research Promotion Project of Nagasaki University Graduate School of Biomedical Sciences (T. Ishikawa); and Fellow-to Faculty Award from American Heart Association (C.J. Jou).

Disclosures

None.

References

1. Mangrum JM, DiMarco JP. The evaluation and management of bradycardia. *N Engl J Med*. 2000;342:703–709. doi: 10.1056/NEJM200003093421006.
2. Benson DW, Wang DW, Dyment M, Knilans TK, Fish FA, Strieper MJ, Rhodes TH, George AL Jr. Congenital sick sinus syndrome caused by recessive mutations in the cardiac sodium channel gene (SCN5A). *J Clin Invest*. 2003;112:1019–1028. doi: 10.1172/JCI18062.
3. Mohler PJ, Splawski I, Napolitano C, Bottelli G, Sharpe L, Timothy K, Priori SG, Keating MT, Bennett V. A cardiac arrhythmia syndrome caused by loss of ankyrin-B function. *Proc Natl Acad Sci U S A*. 2004;101:9137–9142. doi: 10.1073/pnas.0402546101.
4. Nof E, Luria D, Brass D, Marek D, Lahat H, Reznik-Wolf H, Pras E, Dascal N, Eldar M, Glikson M. Point mutation in the HCN4 cardiac ion

channel pore affecting synthesis, trafficking, and functional expression is associated with familial asymptomatic sinus bradycardia. *Circulation.* 2007;116:463–470. doi: 10.1161/CIRCULATIONAHA.107.706887.
5. Amin AS, Asghari-Roodsari A, Tan HL. Cardiac sodium channelopathies. *Pflugers Arch.* 2010;460:223–237. doi: 10.1007/s00424-009-0761-0.
6. Harris SP, Rostkova E, Gautel M, Moss RL. Binding of myosin binding protein-C to myosin subfragment S2 affects contractility independent of a tether mechanism. *Circ Res.* 2004;95:930–936. doi: 10.1161/01.RES.0000147312.02673.56.
7. Granados-Riveron JT, Ghosh TK, Pope M, Bu'Lock F, Thornborough C, Eason J, Kirk EP, Fatkin D, Feneley MP, Harvey RP, Armour JA, David Brook J. Alpha-cardiac myosin heavy chain (MYH6) mutations affecting myofibril formation are associated with congenital heart defects. *Hum Mol Genet.* 2010;19:4007–4016. doi: 10.1093/hmg/ddq315.
8. Gruen M, Gautel M. Mutations in beta-myosin S2 that cause familial hypertrophic cardiomyopathy (FHC) abolish the interaction with the regulatory domain of myosin-binding protein-C. *J Mol Biol.* 1999;286:933–949. doi: 10.1006/jmbi.1998.2522.
9. Reiser PJ, Kline WO. Electrophoretic separation and quantitation of cardiac myosin heavy chain isoforms in eight mammalian species. *Am J Physiol.* 1998;274(3 Pt 2):H1048–H1053.
10. Kimura A. Molecular etiology and pathogenesis of hereditary cardiomyopathy. *Circ J.* 2008;72 Suppl A:A38–A48.
11. Lakdawala NK, Winterfield JR, Funke BH. Dilated cardiomyopathy. *Circ Arrhythm Electrophysiol.* 2013;6:228–237. doi: 10.1161/CIRCEP.111.962050.
12. Carniel E, Taylor MR, Sinagra G, Di Lenarda A, Ku L, Fain PR, Boucek MM, Cavanaugh J, Miocic S, Slavov D, Graw SL, Feiger J, Zhu XZ, Dao D, Ferguson DA, Bristow MR, Mestroni L. Alpha-myosin heavy chain: a sarcomeric gene associated with dilated and hypertrophic phenotypes of cardiomyopathy. *Circulation.* 2005;112:54–59. doi: 10.1161/CIRCULATIONAHA.104.507699.
13. Niimura H, Patton KK, McKenna WJ, Soults J, Maron BJ, Seidman JG, Seidman CE. Sarcomere protein gene mutations in hypertrophic cardiomyopathy of the elderly. *Circulation.* 2002;105:446–451.
14. Ching YH, Ghosh TK, Cross SJ, Packham EA, Honeyman L, Loughna S, Robinson TE, Dearlove AM, Ribas G, Bonser AJ, Thomas NR, Scotter AJ, Caves LS, Tyrrell GP, Newbury-Ecob RA, Munnich A, Bonnet D, Brook JD. Mutation in myosin heavy chain 6 causes atrial septal defect. *Nat Genet.* 2005;37:423–428. doi: 10.1038/ng1526.
15. Posch MG, Waldmuller S, Müller M, Scheffold T, Fournier D, Andrade-Navarro MA, De Geeter B, Guillaumont S, Dauphin C, Youssef D, Schmitt KR, Perrot A, Berger F, Hetzer R, Bouvagnet P, Özcelik C. Cardiac alpha-myosin (MYH6) is the predominant sarcomeric disease gene for familial atrial septal defects. *PLoS One.* 2011;6:e28872. doi: 10.1371/journal.pone.0028872.
16. Arrington CB, Bleyl SB, Matsunami N, Bonnell GD, Otterud BE, Nielsen DC, Stevens J, Levy S, Leppert MF, Bowles NE. Exome analysis of a family with pleiotropic congenital heart disease. *Circ Cardiovasc Genet.* 2012;5:175–182. doi: 10.1161/CIRCGENETICS.111.961797.
17. den Hoed M, Eijgelsheim M, Esko T, Brundel BJ, Peal DS, Evans DM, Nolte IM, Segrè AV, Holm H, Handsaker RE, Westra HJ, Johnson T, Isaacs A, Yang J, Lundby A, Zhao JH, Kim YJ, Go MJ, Almgren P, Bochud M, Boucher G, Cornelis MC, Gudbjartsson D, Hadley D, van der Harst P, Hayward C, den Heijer M, Igl W, Jackson AU, Kutalik Z, Luan J, Kemp JP, Kristiansson K, Ladenvall C, Lorentzon M, Montasser ME, Njajou OT, O'Reilly PF, Padmanabhan S, St Pourcain B, Rankinen T, Salo P, Tanaka T, Timpson NJ, Vitart V, Waite L, Wheeler W, Zhang W, Draisma HH, Feitosa MF, Kerr KF, Lind PA, Mihailov E, Onland-Moret NC, Song C, Weedon MN, Xie W, Yengo L, Absher D, Albert CM, Alonso A, Arking DE, de Bakker PI, Balkau B, Barlassina C, Benaglio P, Bis JC, Bouatia-Naji N, Brage S, Chanock SJ, Chines PS, Chung M, Darbar D, Dina C, Dörr M, Elliott P, Felix SB, Fischer K, Fuchsberger C, de Geus EJ, Goyette P, Gudnason V, Harris TB, Hartikainen AL, Havulinna AS, Heckbert SR, Hicks AA, Hofman A, Holewijn S, Hoogstra-Berends F, Hottenga JJ, Jensen MK, Johansson A, Junttila J, Kääb S, Kanon B, Ketkar S, Khaw KT, Knowles JW, Kooner AS, Kors JA, Kumari M, Milani L, Laiho P, Lakatta EG, Langenberg C, Leusink M, Liu Y, Luben RN, Lunetta KL, Lynch SN, Markus MR, Marques-Vidal P, Mateo Leach I, McArdle WL, McCarroll SA, Medland SE, Miller KA, Montgomery GW, Morrison AC, Müller-Nurasyid M, Navarro P, Nelis M, O'Connell JR, O'Donnell CJ, Ong KK, Newman AB, Peters A, Polasek O, Pouta A, Pramstaller PP, Psaty BM, Rao DC, Ring SM, Rossin EJ, Rudan D, Sanna S, Scott RA, Sehmi JS, Sharp S, Shin JT, Singleton AB, Smith AV, Soranzo N, Spector TD, Stewart C, Stringham HM, Tarasov KV, Uitterlinden AG, Vandenput L, Hwang SJ, Whitfield JB, Wijmenga C, Wild SH, Willemsen G, Wilson JF, Witteman JC, Wong A, Wong Q, Jamshidi Y, Zitting P, Boer JM, Boomsma DI, Borecki IB, van Duijn CM, Ekelund U, Forouhi NG, Froguel P, Hingorani A, Ingelsson E, Kivimaki M, Kronmal RA, Kuh D, Lind L, Martin NG, Oostra BA, Pedersen NL, Quertermous T, Rotter JI, van der Schouw YT, Verschuren WM, Walker M, Albanes D, Arnar DO, Assimes TL, Bandinelli S, Boehnke M, de Boer RA, Bouchard C, Caulfield WL, Chambers JC, Curhan G, Cusi D, Eriksson J, Ferrucci L, van Gilst WH, Glorioso N, de Graaf J, Groop L, Gyllensten U, Hsueh WC, Hu FB, Huikuri HV, Hunter DJ, Iribarren C, Isomaa B, Jarvelin MR, Jula A, Kähönen M, Kiemeney LA, van der Klauw MM, Kooner JS, Kraft P, Iacoviello L, Lehtimäki T, Lokki ML, Mitchell BD, Navis G, Nieminen MS, Ohlsson C, Poulter NR, Qi L, Raitakari OT, Rimm EB, Rioux JD, Rizzi F, Rudan I, Salomaa V, Sever PS, Shields DC, Shuldiner AR, Sinisalo J, Stanton AV, Stolk RP, Strachan DP, Tardif JC, Thorsteinsdottir U, Tuomilehto J, van Veldhuisen DJ, Virtamo J, Viikari J, Vollenweider P, Waeber G, Widen E, Cho YS, Olsen JV, Visscher PM, Willer C, Franke L, Erdmann J, Thompson JR, Pfeufer A, Sotoodehnia N, Newton-Cheh C, Ellinor PT, Stricker BH, Metspalu A, Perola M, Beckmann JS, Smith GD, Stefansson K, Wareham NJ, Munroe PB, Sibon OC, Milan DJ, Snieder H, Samani NJ, Loos RJ; Global BPgen Consortium; CARDIoGRAM Consortium; PR GWAS Consortium; QRS GWAS Consortium; QT-IGC Consortium; CHARGE-AF Consortium. Identification of heart rate-associated loci and their effects on cardiac conduction and rhythm disorders. *Nat Genet.* 2013;45:621–631. doi: 10.1038/ng.2610.
18. Holm H, Gudbjartsson DF, Arnar DO, Thorleifsson G, Thorgeirsson G, Stefansdottir H, Gudjonsson SA, Jonasdottir A, Mathiesen EB, Njølstad I, Nyrnes A, Wilsgaard T, Hald EM, Hveem K, Stoltenberg C, Løchen ML, Kong A, Thorsteinsdottir U, Stefansson K. Several common variants modulate heart rate, PR interval and QRS duration. *Nat Genet.* 2010;42:117–122. doi: 10.1038/ng.511.
19. Eijgelsheim M, Newton-Cheh C, Sotoodehnia N, de Bakker PI, Müller M, Morrison AC, Smith AV, Isaacs A, Sanna S, Dörr M, Navarro P, Fuchsberger C, Nolte IM, de Geus EJ, Estrada K, Hwang SJ, Bis JC, Rückert IM, Alonso A, Launer LJ, Hottenga JJ, Rivadeneira F, Noseworthy PA, Rice KM, Perz S, Arking DE, Spector TD, Kors JA, Aulchenko YS, Tarasov KV, Homuth G, Wild SH, Marroni F, Gieger C, Licht CM, Prineas RJ, Hofman A, Rotter JI, Hicks AA, Ernst F, Najjar SS, Wright AF, Peters A, Fox ER, Oostra BA, Kroemer HK, Couper D, Völzke H, Campbell H, Meitinger T, Uda M, Witteman JC, Psaty BM, Wichmann HE, Harris TB, Kääb S, Siscovick DS, Jamshidi Y, Uitterlinden AG, Folsom AR, Larson MG, Wilson JF, Penninx BW, Snieder H, Pramstaller PP, van Duijn CM, Lakatta EG, Felix SB, Gudnason V, Pfeufer A, Heckbert SR, Stricker BH, Boerwinkle E, O'Donnell CJ. Genome-wide association analysis identifies multiple loci related to resting heart rate. *Hum Mol Genet.* 2010;19:3885–3894. doi: 10.1093/hmg/ddq303.
20. Holm H, Gudbjartsson DF, Sulem P, Masson G, Helgadottir HT, Zanon C, Magnusson OT, Helgason A, Saemundsdottir J, Gylfason A, Stefansdottir H, Gretarsdottir S, Matthiasson SE, Thorgeirsson GM, Jonasdottir A, Sigurdsson A, Stefansson H, Werge T, Rafnar T, Kiemeney LA, Parvez B, Muhammad R, Roden DM, Darbar D, Thorleifsson G, Walters GB, Kong A, Thorsteinsdottir U, Arnar DO, Stefansson K. A rare variant in MYH6 is associated with high risk of sick sinus syndrome. *Nat Genet.* 2011;43:316–320. doi: 10.1038/ng.781.
21. Singleman C, Holtzman NG. Analysis of postembryonic heart development and maturation in the zebrafish, Danio rerio. *Dev Dyn.* 2012;241:1993–2004. doi: 10.1002/dvdy.23882.
22. Abe K, Machida T, Sumitomo N, Yamamoto H, Ohkubo K, Watanabe I, Makiyama T, Fukae S, Kohno M, Harrell DT, Ishikawa T, Tsuji Y, Nogami A, Watabe T, Oginosawa Y, Abe H, Maemura K, Motomura H, Makita N. Sodium channelopathy underlying familial sick sinus syndrome with early onset and predominantly male characteristics. *Circ Arrhythm Electrophysiol.* 2014;7:511–517. doi: 10.1161/CIRCEP.113.001340.
23. Turner DL, Weintraub H. Expression of achaete-scute homolog 3 in Xenopus embryos converts ectodermal cells to a neural fate. *Genes Dev.* 1994;8:1434–1447.
24. Rupp RA, Snider L, Weintraub H. Xenopus embryos regulate the nuclear localization of XMyoD. *Genes Dev.* 1994;8:1311–1323.
25. Arimura T, Ishikawa T, Nunoda S, Kawai S, Kimura A. Dilated cardiomyopathy-associated BAG3 mutations impair Z-disc assembly and enhance sensitivity to apoptosis in cardiomyocytes. *Hum Mutat.* 2011;32:1481–1491. doi: 10.1002/humu.21603.
26. White SM, Constantin PE, Claycomb WC. Cardiac physiology at the cellular level: use of cultured HL-1 cardiomyocytes for studies of cardiac muscle cell structure and function. *Am J Physiol Heart Circ Physiol.* 2004;286:H823–H829. doi: 10.1152/ajpheart.00986.2003.

27. Berdougo E, Coleman H, Lee DH, Stainier DY, Yelon D. Mutation of weak atrium/atrial myosin heavy chain disrupts atrial function and influences ventricular morphogenesis in zebrafish. *Development*. 2003;130:6121–6129. doi: 10.1242/dev.00838.
28. Kimmel CB, Ballard WW, Kimmel SR, Ullmann B, Schilling TF. Stages of embryonic development of the zebrafish. *Dev Dyn*. 1995;203:253–310. doi: 10.1002/aja.1002030302.
29. Kunst G, Kress KR, Gruen M, Uttenweiler D, Gautel M, Fink RH. Myosin binding protein C, a phosphorylation-dependent force regulator in muscle that controls the attachment of myosin heads by its interaction with myosin S2. *Circ Res*. 2000;86:51–58.
30. Palmer BM, Georgakopoulos D, Janssen PM, Wang Y, Alpert NR, Belardi DF, Harris SP, Moss RL, Burgon PG, Seidman CE, Seidman JG, Maughan DW, Kass DA. Role of cardiac myosin binding protein C in sustaining left ventricular systolic stiffening. *Circ Res*. 2004;94:1249–1255. doi: 10.1161/01.RES.0000126898.95550.31.
31. Hughes SE, McKenna WJ. New insights into the pathology of inherited cardiomyopathy. *Heart*. 2005;91:257–264. doi: 10.1136/hrt.2004.040337.
32. Bahrudin U, Morikawa K, Takeuchi A, Kurata Y, Miake J, Mizuta E, Adachi K, Higaki K, Yamamoto Y, Shirayoshi Y, Yoshida A, Kato M, Yamamoto K, Nanba E, Morisaki H, Morisaki T, Matsuoka S, Ninomiya H, Hisatome I. Impairment of ubiquitin-proteasome system by E334K cMyBPC modifies channel proteins, leading to electrophysiological dysfunction. *J Mol Biol*. 2011;413:857–878. doi: 10.1016/j.jmb.2011.09.006.
33. Chandler NJ, Greener ID, Tellez JO, Inada S, Musa H, Molenaar P, Difrancesco D, Baruscotti M, Longhi R, Anderson RH, Billeter R, Sharma V, Sigg DC, Boyett MR, Dobrzynski H. Molecular architecture of the human sinus node: insights into the function of the cardiac pacemaker. *Circulation*. 2009;119:1562–1575. doi: 10.1161/CIRCULATIONAHA.108.804369.
34. Yamamoto M, Dobrzynski H, Tellez J, Niwa R, Billeter R, Honjo H, Kodama I, Boyett MR. Extended atrial conduction system characterised by the expression of the HCN4 channel and connexin45. *Cardiovasc Res*. 2006;72:271–281. doi: 10.1016/j.cardiores.2006.07.026.
35. Anan R, Greve G, Thierfelder L, Watkins H, McKenna WJ, Solomon S, Vecchio C, Shono H, Nakao S, Tanaka H. Prognostic implications of novel beta cardiac myosin heavy chain gene mutations that cause familial hypertrophic cardiomyopathy. *J Clin Invest*. 1994;93:280–285. doi: 10.1172/JCI116957.

Circulation
Arrhythmia and Electrophysiology

American Heart Association®

Novel Mutation in the α-Myosin Heavy Chain Gene Is Associated With Sick Sinus Syndrome

Taisuke Ishikawa, Chuanchau J. Jou, Akihiko Nogami, Shinya Kowase, Cammon B. Arrington, Spencer M. Barnett, Daniel T. Harrell, Takuro Arimura, Yukiomi Tsuji, Akinori Kimura and Naomasa Makita

Circ Arrhythm Electrophysiol. 2015;8:400-408; originally published online February 25, 2015;
doi: 10.1161/CIRCEP.114.002534
Circulation: Arrhythmia and Electrophysiology is published by the American Heart Association, 7272 Greenville Avenue, Dallas, TX 75231

Print ISSN: 1941-3149. Online ISSN: 1941-3084

Journal of Cardiology xxx (2015) xxx–xxx

Contents lists available at ScienceDirect

Journal of Cardiology

journal homepage: www.elsevier.com/locate/jjcc

Original article

LMNA cardiomyopathy detected in Japanese arrhythmogenic right ventricular cardiomyopathy cohort

Koichi Kato (MD, PhD)[a], Naohiko Takahashi (MD, PhD)[b], Yusuke Fujii (MD)[a], Aya Umehara (DVM)[c], Suguru Nishiuchi (MD)[c], Takeru Makiyama (MD, PhD)[c], Seiko Ohno (MD, PhD)[a], Minoru Horie (MD, PhD)[a,*]

[a] *Department of Cardiovascular and Respiratory Medicine, Shiga University of Medical Science, Shiga, Japan*
[b] *Department of Cardiology and Clinical Examination, Faculty of Medicine, Oita University, Oita, Japan*
[c] *Department of Cardiovascular Medicine, Kyoto University Graduate School of Medicine, Kyoto, Japan*

ARTICLE INFO

Article history:
Received 19 May 2015
Received in revised form 1 October 2015
Accepted 5 October 2015
Available online xxx

Keywords:
LMNA
Arrhythmogenic right ventricular cardiomyopathy
Desmosome
PKP2
Pacemaker therapy

ABSTRACT

Background: Arrhythmogenic right ventricular cardiomyopathy (ARVC) is an inherited cardiac disease. While desmosomal gene mutations are considered major causes of ARVC, *LMNA* mutations have been reported to be possible causes of ARVC. In this study, we performed extensive genetic screening for *LMNA* mutations in our Japanese ARVC cohort to assess the prevalence and characteristics of *LMNA* mutation-positive ARVC cases.
Methods: Our study cohort consisted of 57 ARVC probands. Genetic analyses were performed by using direct sequencing and targeted sequencing of *LMNA* and four desmosomal genes. We compared clinical features of probands with desmosomal gene mutations to those of probands with *LMNA* mutations.
Results: Among 57 clinically diagnosed ARVC probands, we identified desmosomal gene mutations in 26 probands (45.6%) and two *LMNA* mutations in two probands. The first *LMNA* mutation p.M1K was detected in a 62-year-old male proband, while the second mutation p.W514X was found in a 70-year-old male proband. Compared to the 26 probands with desmosomal gene mutations, in the two probands with *LMNA* mutations, the mean age at diagnosis was significantly higher, and their heart rate at the diagnosis was significantly slower. While both probands with *LMNA* mutations underwent pacemaker implantation, only one proband with desmosomal mutations received this treatment (2/2 vs. 1/26).
Conclusion: Genetic screening for *LMNA* gene is important for ARVC patients, particularly in patients with bradycardia.

Introduction

Arrhythmogenic right ventricular cardiomyopathy (ARVC) is a disease characterized by fibrofatty replacement in the right ventricular myocardium and ventricular arrhythmia [1]. The disease expression varies widely from sudden cardiac death to severe heart failure which sometimes requires heart transplantation [2]. Recognition of arrhythmogenic left ventricular cardiomyopathy (ALVC) [3,4] and biventricular involving subtype has led to a more comprehensive definition of this disease entity. The term "arrhythmogenic cardiomyopathy (AC)" has been proposed [5]. Mutations in desmosomal protein genes have been shown to be a major cause of AC [6–8]. However, causative mutations in those genes could only be identified in 40–60% of patients [9,10]. Mutations of the *LMNA* gene have been associated with a variety of systemic diseases such as Hutchinson-Gilford progeria [11], dystrophy [12], and dilated cardiomyopathy [13]. A study conducted in England indicated that several *LMNA* mutations are clinically associated with ARVC. The authors screened 108 ARVC probands and found four *LMNA* mutation carriers (4%), suggesting *LMNA* as a new causative gene of ARVC [14]. Meanwhile, a Canadian team reported a case of *LMNA* mutation cardiomyopathy with features of ARVC [15].

In this study, we surveyed ARVC probands in our genetic database for *LMNA* mutations and compared clinical features of *LMNA* mutation carriers with those of desmosomal gene mutation carriers.

* Corresponding author at: Department of Cardiovascular and Respiratory Medicine, Shiga University of Medical Science, Seta-Tsukinowa, Otsu, Shiga 520-2192, Japan. Tel.: +81 77 548 2213; fax: +81 77 543 5839.
E-mail address: horie@belle.shiga-med.ac.jp (M. Horie).

http://dx.doi.org/10.1016/j.jjcc.2015.10.013
0914-5087/

Please cite this article in press as: Kato K, et al. *LMNA* cardiomyopathy detected in Japanese arrhythmogenic right ventricular cardiomyopathy cohort. J Cardiol (2015), http://dx.doi.org/10.1016/j.jjcc.2015.10.013

Methods

Genetic analysis

Our study cohort consisted of 57 ARVC probands who were referred to our institute for genetic screening. The diagnosis of ARVC was based on the International Task Force Criteria for ARVC (2010) [16]. After obtaining written informed consent, genomic DNA was isolated from peripheral blood lymphocytes. Coding exons of *LMNA*, four desmosomal protein genes (*PKP2*, *DSP*, *DSG2*, and *DSC*), and three major LQTS-related genes (*KCNQ1*, *KCNH2*, and *SCN5A*) were amplified and sequenced using an ABI PRISM-3130 DNA sequencer (Applied Biosystems, Foster City, CA, USA). Among mutation-negative probands, some had apparent family histories of ARVC. In such a case, we used a personal next generation sequencer (Illumina®, San Diego, CA, USA) to analyze desmosomal protein genes and *LMNA* again, by method of targeted gene sequencing. The genetic variants identified were probed in 100 ethnically matched control population (200 alleles) and in two available online databases (http://evs.gs.washington.edu/and http://www.1000genomes.org/). The protocol for the genetic test was approved by the institutional ethics committee and was performed under its guidelines. We assessed the deleteriousness of detected variants by using Combined Annotation Dependent Depletion (CADD, http://cadd.gs.washington.edu/home) [17]. Variants with scaled C-score of greater or equal 20 were considered deleterious.

Comparison of clinical features

Compatibility with the International Task Force Criteria for ARVC (2010) [16] was assessed for patients with desmosomal protein genes ($n = 26$) and for those with *LMNA* mutations ($n = 2$). For this comparison, we used clinical data obtained by echocardiogram and 12-lead electrocardiogram (ECG). Findings from other tests such as cardiac magnetic resonance imaging (MRI), computed tomography (CT) imaging, tissue biopsy, and signal-averaged ECG were not compared because they were not performed for all probands in our cohort. Using Student's *t*-test for continuous variables, and Fisher's exact test for nominal variables, differences were considered statistically significant at $p < 0.05$. Data are presented as mean ± SD.

Results

ARVC cohort and the International Task Force Criteria for ARVC (2010)

Table 1 summarizes the number of the probands, who are carrying genetic variants in genes we screened, and the compatibility with the International Task Force Criteria for ARVC (2010) [16]. We identified two *LMNA* mutations in two probands, one *SCN5A* mutation in one proband, and 21 desmosomal gene mutations in 26 probands. Consequently, 28 probands were negative for the genes screened (49.1%). Desmosomal gene mutations were most frequently identified as mutations in *PKP2* (12 cases). Three probands had compound mutations in two different desmosomal genes.

Table 1
The summary of results of genetic screening and the compatibility of the International Task Force Criteria for arrhythmogenic right ventricular cardiomyopathy [16].

	Definite	Border	Possible	Total
Genes				
PKP2	11	0	0	11
DSP	3	0	0	3
DSG2	7	0	0	7
DSC2	1	0	0	1
DSP+DSG2	2	0	0	2
PKP2+DSP	1	0	0	1
DSG2+SCN5A	1	0	0	1
LMNA	2	0	0	2
SCN5A	0	1	0	1
Non-genotyped	17	10	1	28
Total	45	11	1	57

Case 1: LMNA p.M1K mutation

A male proband first presented with atrial fibrillation and complete atrioventricular block in his fifties. His QRS duration progressively widened and atrial contraction weakened over the following 20 years. When he was hospitalized for dyspnea on effort at age 70 years, his resting ECG showed sinus arrest and junctional irregular rhythm with wide QRS, while echocardiography and CT imaging showed severe RV and mild LV dilatation (Figs. 1 and 2A). Localized RV dyskinesis was apparent in RV apex (Fig. 1B). Holter ECG revealed frequent premature ventricular contractions and non-sustained ventricular tachycardia. His low cardiac function and bradyarrhythmia with wide QRS required a cardiac resynchronization therapy device implantation. He was diagnosed with ARVC, based on the International Task Force Criteria for ARVC [16] (two major and one minor criteria: structural alterations, family history, and arrhythmia). Genetic analysis of his DNA revealed a mutation in *LMNA*, namely p.M1K (c.2T>A, Fig. 2B) in a heterozygous fashion. In available online databases and 100 ethnically matched control population, we could not identify the same mutation. CADD score of this variant was 28, which suggested the possibility that the variant caused his disease (Table 2, Case 1).

Family members with LMNA p.M1K mutation

The pedigree is shown in Fig. 2C. The proband's brother had undergone pacemaker implantation and died from severe heart failure with RV dilatation in his sixties (II:3). While no DNA sample from the proband's brother was available, the same mutation was detected in his daughter (III:4), indicating that the deceased brother was an obligatory mutation carrier. The daughter (III:4, aged 42 years) had normal ECG and normal echocardiographic findings. In addition, the proband's daughter and son (III:1 and III:2, aged 47 and 40 years, respectively), and his half-brother (II:5, aged 54 years) had the same mutation. The proband's son had polymorphic premature ventricular contractions with normal cardiac function and normal chamber size (III:2). Other mutation positive members, the proband's half-brother (II:5), the proband's daughter (III:1), and the proband's brother's daughter (III:4), did not show ECG and echocardiographic abnormalities.

Table 2
Genetic screening result of two LMNA mutation cases and analyses of deleteriousnesss.

	Case 1	Case 2
LMNA	2T > A	1542G > A
PKP2	–	–
DSP	–	–
DSG2	–	–
DSC2	–	–
KCNQ1	–	–
KCNH2	–	–
SCN5A	–	–
Polyphen-2	0.055	NA
CADD score	28	42

NA, not available.

Please cite this article in press as: Kato K, et al. *LMNA* cardiomyopathy detected in Japanese arrhythmogenic right ventricular cardiomyopathy cohort. J Cardiol (2015), http://dx.doi.org/10.1016/j.jjcc.2015.10.013

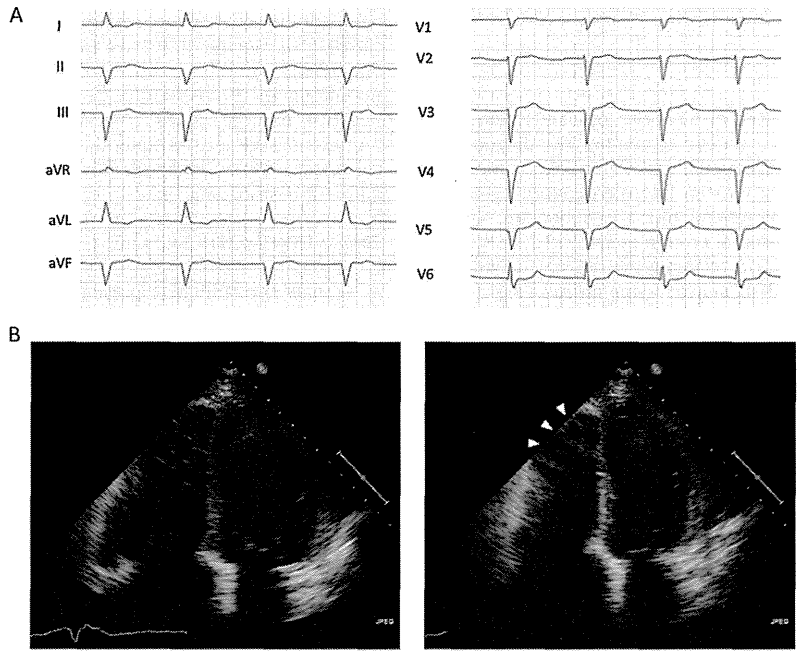

Fig. 1. Electrocardiogram and echocardiogram of *LMNA* p.M1K mutation carrier. (Panel A) Electrocardiogram of the proband in his sixties. (Panel B) Echocardiographic image showing diastolic (left) and systolic phase (right) of both ventricles. Right ventricle (RV) shows focal akinesis in apex area (arrow heads). The lateral basal area of RV keeps its contraction.

Case 2: LMNA *p.W514X mutation*

A male proband was first hospitalized for atrial standstill and complete atrioventricular block at age 62 years (Fig. 3A left panel). A part of this proband's clinical information was previously reported [18]. His RV and right atrium (RA) were remarkably dilated, and an RV endomyocardial biopsy demonstrated fibrous tissue replacement of the myocardium (Fig. 3B). In addition, his

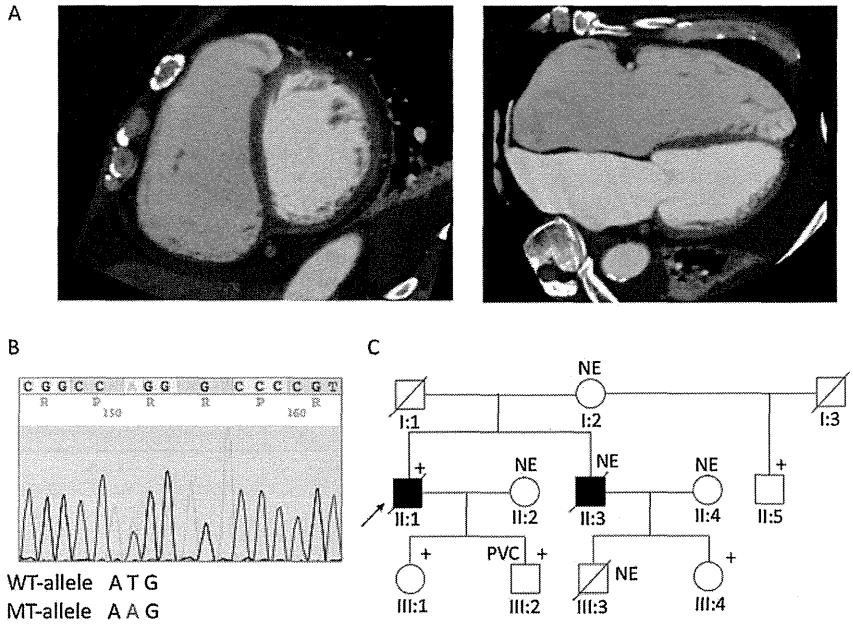

Fig. 2. Computed tomography (CT) images and genetic analysis of *LMNA* p.M1K mutation carriers. (Panel A) CT scanning image showing dilated right atrium and ventricle. (Panel B) Proband's original sequence of *LMNA* showing a heterozygous mutation in exon1, replacing the first codon of the gene (ATG) with AAG. (Panel C) Pedigree of the *LMNA* p.M1K mutation family. Arrow indicates the proband. Filled symbols indicate members affected by clinical phenotypes. Plus signs indicate mutation positive. NE = not examined.

Please cite this article in press as: Kato K, et al. *LMNA* cardiomyopathy detected in Japanese arrhythmogenic right ventricular cardiomyopathy cohort. J Cardiol (2015), http://dx.doi.org/10.1016/j.jjcc.2015.10.013

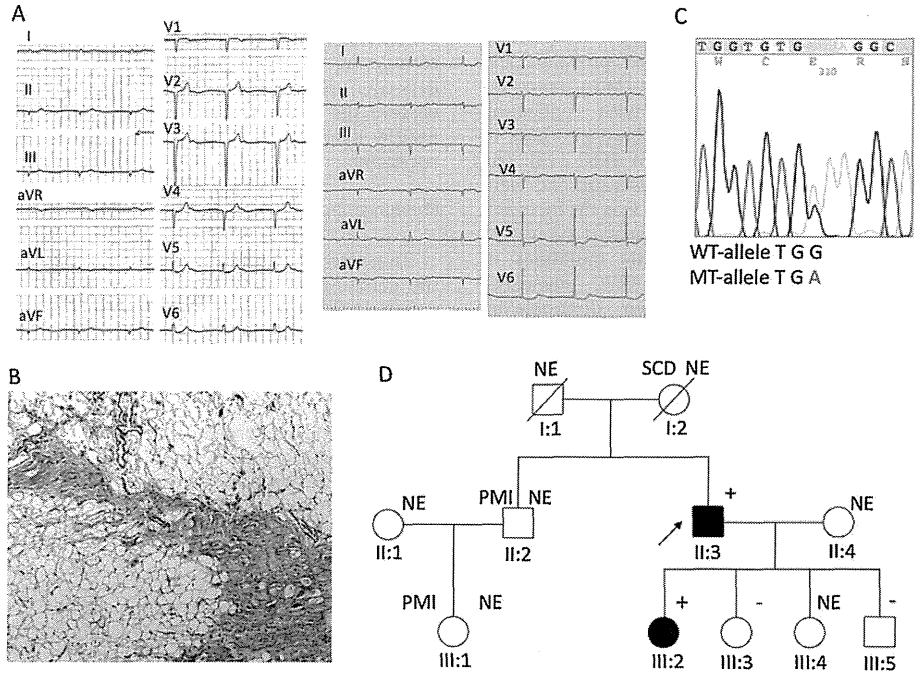

Fig. 3. Clinical information and genetic analysis of *LMNA* p.W514X mutation carriers. (Panel A) Electrocardiogram of the proband at age 62 years (left) and that of the proband's 45-year-old daughter (right) carrying the same mutation as that in the proband. (Panel B) Histological example of right ventricular myocardium, showing loss of cardiomyocyte and fibrous tissue replacement. Slightly high power view. (Panel C) Proband's original sequence of *LMNA* showing a heterozygous mutation in exon 8. (Panel D) Pedigree of the *LMNA* p.W514X family. Arrow indicates the proband. Closed symbols indicate members affected by clinical phenotypes. Plus signs indicate mutation-positive individuals. PMI = pacemaker implanted; NE = not examined.

left ventricular (LV) function was moderately reduced (ejection fraction 33%), and he developed recurrent ventricular tachycardia (VT) with a left bundle branch block morphology, requiring implantable cardioverter defibrillator (ICD) implantation at age 70 years. Based on the International Task Force Criteria for ARVC [16], he was diagnosed as having ARVC (three major criteria: tissue characteristics, structural alterations, and arrhythmia). Genetic testing identified a heterozygous p.W514X (c.1542G>A) mutation in exon 8 of *LMNA* (Fig. 3C), but was negative for mutations in the four ARVC-related desmosomal gene described above. In available online databases and 100 ethnically matched control population, *LMNA* c.1542G>A was not identified. The CADD score of this variant was 42, suggesting this mutation could cause the disease (Table 2: Case 2).

Family members with LMNA *p.W514X mutation*

The pedigree is shown in Fig. 3D. The proband's mother (I:2) died suddenly in her forties, and both of the proband's elder brother (II:2) and the brother's daughter (III:1) had pacemaker implantations; detailed information could not be obtained because they lived abroad. The proband's two daughters and son underwent genetic analysis, ECG measurement, and echocardiographic examination. The eldest, a 45-year-old daughter (III:2), was found to carry the same heterozygous p.W514X *LMNA* mutation. She had atrial fibrillation with AV conduction disturbance, but remained asymptomatic (Fig. 3A, right panel). Her echocardiographic findings revealed dilatation of RA and RV, compatible to that observed in ARVC. Moderate tricuspid and mild mitral valve regurgitation were also recognized, while her LV systolic function was normal (ejection fraction >60%). The two other genotype-negative siblings showed no electrocardiographic abnormalities (III:3, III:5).

Comparison between the characteristics of LMNA *mutation carriers and those of desmosomal gene mutation carriers (Table 3)*

Table 3 shows characteristics of desmosomal gene mutation carriers and *LMNA* mutation carriers. Because of atrioventricular conduction disturbance, heart rate was significantly slower, and pacemaker therapy was relatively more necessary in *LMNA* mutation carriers than in desmosomal gene mutation carriers. The age of diagnosis was significantly higher in *LMNA* mutation carriers than in desmosomal gene mutation carriers (66 ± 5.7 years vs. 40.5 ± 19.9 years, $p = 0.01$). Although the difference was not significant, epsilon waves, and inverted T waves in right precordial leads, which are specific electrocardiographic signs of ARVC, were absent in the two *LMNA* mutation carriers.

Table 3
Comparison of desmosomal arrhythmogenic right ventricular cardiomyopathy (ARVC) vs. *LMNA* positive ARVC cases.

	Desmosomal mutation	*LMNA* mutation
Number of probands (male)	26 (17)	2 (2)
Age at diagnosis (years)	40.5 ± 19.9	66 ± 5.7*
Heart rate	60.6 ± 12.5	45 ± 1.4*
Pacemaker implantation	1 (4%)	2* (67%)
Compatibility of diagnostic criteria		
RV dilatation by UCG	20 (77%)	2 (67%)
Inverted T waves	9 (36%)	0
Epsilon wave	4 (15%)	0
LBBB type VT	6 (23%)	1 (33%)

* $p < 0.05$.

Please cite this article in press as: Kato K, et al. *LMNA* cardiomyopathy detected in Japanese arrhythmogenic right ventricular cardiomyopathy cohort. J Cardiol (2015), http://dx.doi.org/10.1016/j.jjcc.2015.10.013

Discussion

In this study, we surveyed 57 Japanese ARVC probands, and identified two probands carrying heterozygous *LMNA* mutations who displayed ARVC-like cardiomyopathy with conduction disturbance. The disease concept of ARVC can be traced back to the summary of 24 cases by Marcus et al. in 1982 [19]. The diagnostic criteria were first published in 1994 [20], and were revised in 2010 [16]. One of the major revisions was the inclusion of genetic factors as a major criterion. This change was introduced owing to the recent identification of genetic mutations in desmosome-related protein genes underlying ARVC. Nowadays, five desmosome-related proteins, plakoglobin, desmoplakin, plakophilin-2, desmoglein-2, and desmocollion-2, have been associated with ARVC, and mutations in these genes are detected in approximately 40–50% of ARVC cases [9,10]. In addition to them, current systematic genetic analyses have identified several non-desmosomal gene mutations in families with ARVC, although their prevalence is low. To date, TGFβ3 [21], DES [22], TMEM43 [23], PLN [24], CTNNA3, and TTN [25] have been associated with ARVC. However, the genetic background of a considerable number of ARVC cases remains unclear.

LMNA is a gene encoding lamin, a structural protein of the nuclear envelope. Mutations in this gene cause a variety of systemic diseases that are commonly called laminopathy. Laminopathy is associated with several tissues such as striated muscles, peripheral nerves, and adipose tissues. Emery-Dreifuss muscular dystrophy (EDMD) [11] and dilated cardiomyopathy [12] are known as major striated muscle laminopathies, which account for more than 50% of laminopathy cases [26]. Systemically, a premature-aging syndrome such as Hutchinson-Gilford progeria syndrome is a known clinical manifestation of laminopathy. In 2012, Quarta et al. reported on four families with *LMNA* mutations mimicking ARVC-like phenotypes [14]. They screened 108 ARVC cases for desmosomal protein genes and *LMNA*, and detected desmosomal gene mutations in 61 cases (56.5%) and *LMNA* mutations in 4 (4%) cases, suggesting the possibility of *LMNA* mutations being causative factors of ARVC. However, so far, only one case report by a Canadian group [15] has followed this study. In our study, we found two *LMNA* mutation cases in a Japanese ARVC cohort. Additionally, we identified several clinical features to distinguish these ARVC-mimicking cases from "classical ARVC" cases. Clinically, both desmosomal and *LMNA*-related ARVC were identified by their VT events or remarkable RV enlargement on echocardiography. On the other hand, typical electrocardiographic features such as epsilon waves and inverted T waves in right precordial leads are rare in *LMNA* cases. Instead, QRS widening and atrioventricular conduction disturbance were frequently observed in *LMNA* mutation-positive ARVC cases. Such ECG results were also reported by Quarta et al. [14], and shared common features with laminopathy DCM [13]. Therefore, it is not difficult to distinguish *LMNA* mutation-positive ARVC cases from classical desmosomal gene mutation-positive ARVC by careful assessment of clinical characteristics.

The cosegregation and phenotype-genotype correlation in LMNA *p.M1K mutation family*

The penetrance of lamin-cardiomyopathy is not 100%, and varies widely, sometimes gender specifically. Arimura et al. [27] reported the association of androgen receptor and disease progression of lamin cardiomyopathy. In the study, they introduced severe phenotype expression in male cases. In our study, younger generation of family members carrying *LMNA* c.2T>A mutation (Fig. 2C generation III) seems to have no apparent signs of cardiomyopathy. And case II:5 (Fig. 2C), who is currently in his fifties, does not have any signs of cardiomyopathy. However, considering its gender-specific phenotype expression and age-dependent progression, there is still a considerable possibility to observe the expression of cardiomyopathy in these apparently healthy members in the following decades. Careful follow-up is necessary.

Combined annotation dependent deletion

To assess the deleteriousness of detected variants, we employed the combined annotation dependent deletion (CADD) scoring system [17]. This system ranked all ~8.6 billion single nucleotide variants of the GRCh37/hg19 reference and scored "PHRED-like scaled C-scores" to each variant. A scaled C-score of greater or equal to 10 indicates that these are predicted to be the 10% most deleterious substitutions, a score of greater or equal to 20 indicates the 1% most deleterious and so on. To apply a cutoff on deleteriousness, we put a cutoff value at 20, which indicates the substitution is the rarest 1% in all possible variants.

Japanese ARVC cohort and arrhythmogenic cardiomyopathy

The disease expression of ARVC families widely varies. In addition to classical RV pattern, some show left dominant pattern and others show biventricular involvement. These days, the term "arrhythmogenic cardiomyopathy (AC)" [5] has been proposed to indicate a more comprehensive concept by some authors. However, so far, there is still not a systematic diagnostic guideline for AC, and left dominant AC cases tend to be missed or misdiagnosed as dilated cardiomyopathy in clinical settings. Our Japanese ARVC cohort also has this problem. It contains mainly classic ARVC cases, but some biventricular involvement subtypes, and a few end-stage ALVC cases are included. Actually in cases carrying *LMNA* mutations, p.M1K mutation positive proband is suspected to be a AC with biventricular involvement. In future study, AC should be diagnosed more systematically, and mixed cohort of different disease expressions should be more carefully assessed. However at this moment, this mixed study cohort represents Japanese ARVC cases in the actual clinical situation.

Conclusion

Genetic screening of *LMNA* is an important diagnostic option for late onset ARVC with bradyarrhythmia. Careful assessment of electrocardiographic information is key to predicting associations of *LMNA* gene mutation.

Funding

This work was supported by research grants from the Ministry of Education, Culture, Science, and Technology of Japan, and health science research grants from the Ministry of Health, Labor and Welfare of Japan for Clinical Research on Measures for Intractable Diseases.

Conflict of interest

All authors have no conflict of interest to disclose.

Acknowledgments

A part of this article has been presented at the 63rd American College of Cardiology Annual Scientific Session in 2014.

Please cite this article in press as: Kato K, et al. *LMNA* cardiomyopathy detected in Japanese arrhythmogenic right ventricular cardiomyopathy cohort. J Cardiol (2015), http://dx.doi.org/10.1016/j.jjcc.2015.10.013

References

[1] Awad MM, Calkins H, Judge DP. Mechanisms of disease: molecular genetics of arrhythmogenic right ventricular dysplagia/cardiomyopathy. Nat Clin Pract Cardiovasc Med 2008;5:258–67.
[2] Chung FP, Lin YJ, Chang SL, Lo LW, Hu YF, Tuan TC, Chao TF, Liao JN, Chiou CW, Chen SA. Current and state of the art on the electrophysiologic characteristics and catheter ablation of arrhythmogenic right ventricular dysplasia/cardiomyopathy. J Cardiol 2015;65:441–50.
[3] Norman M, Simpson M, Mogensen J, Shaw A, Hughes S, Syrris P, Sen-Chowdhry S, Rowland E, Crosby A, McKenna WJ. Novel mutation in desmoplakin causes arrhythmogenic left ventricular cardiomyopathy. Circulation 2005;112:636–42.
[4] Sen-Chowdhry S, Syrris P, Prasad SK, Hughes SE, Merrifield R, Ward D, Pennell DJ, McKenna WJ. Left-dominant arrhythmogenic cardiomyopathy: an underrecognized clinical entity. J Am Coll Cardiol 2008;52:2175–87.
[5] Sen-Chowdhry S, Morgan RD, Chambers JC, McKenna WJ. Arrhythmogenic cardiomyopathy: etiology, diagnosis, and treatment. Annu Rev Med 2010;61:233–53.
[6] McKoy G, Protonotarios N, Crosby A, Tsatsopoulou A, Anastasakis A, Coona A, Norman M, Baboonian C, Jeffery S, McKenna WJ. Identification of a deletion in plakoglobin in arrhythmogenic right ventricular cardiomyopathy with palmoplantar keratoderma and wooly hair (Naxos disease). Lancet 2000;355:2119–24.
[7] Norgett EE, Hatsell SJ, Carvajal-Huerta L, Cabezas JC, Common J, Purkis PE, Whittock N, Leigh IM, Stevens HP, Kelsell DP. Recessive mutation in desmoplakin disrupts desmoplakin-intermediate filament interactions and causes dilated cardiomyopathy, woolly hair and keratoderma. Hum Mol Genet 2000;9:2761–6.
[8] Gerull B, Heuser A, Wichter T, Paul M, Basson CT, McDermott DA, Lerman BB, Markowitz SM, Ellinor PT, MacRae CA, Peters S, Grossmann KS, Drenckhahn J, Michely B, Sasse-Klaassen S, et al. Mutations in the desmosomal protein plakophilin-2 are common in arrhythmogenic right ventricular cardiomyopathy. Nat Genet 2004;36:1162–4.
[9] Ohno S, Nagaoka I, Fukuyama M, Kimura H, Itoh H, Makiyama T, Shimizu A, Horie M. Age-dependent clinical and genetic characteristics in Japanese patients with arrhythmogenic right ventricular cardiomyopathy/dysplasia. Circ J 2013;77:1534–42.
[10] Fressart V, Duthoit G, Donal E, Probst V, Deharo JC, Chevalier P, Klug D, Dubourg O, Delacretaz E, Cosnay P, Scanu P, Extramiana F, Keller D, Hidden-Lucet F, Simon F, et al. Desmosomal gene analysis in arrhythmogenic right ventricular dysplasia/cardiomyopathy: spectrum of mutations and clinical impact in practice. Europace 2010;12:861–8.
[11] De Sandre-Giovannoli A, Bernard R, Cau P, Navarro C, Amiel J, Boccaccio I, Lyonnet S, Stewart CL, Munnich A, Le Merrer M, Lévy N. Lamin A truncation in Hutchinson-Gilford progeria. Science 2003;300:2055.
[12] Bonne G, Di Barletta MR, Varnous S, Bécane HM, Hammouda EH, Merlini L, Muntoni F, Greenberg CR, Gary F, Urtizberea JA, Duboc D, Fardeau M, Toniolo D, Schwartz K. Mutations in the gene encoding lamin A/C cause autosomal dominant Emary-Dreifuss muscular dystrophy. Nat Genet 1999;21:285–8.
[13] Fatkin D, MacRae C, Sasaki T, Wolff MR, Porcu M, Frenneaux M, Atherton J, Vidaillet Jr HJ, Spudich S, De Girolami U, Seidman JG, Seidman C, Muntoni F, Müehle G, Johnson W, et al. Missense mutations in the rod domain of the lamin A/C gene as causes of dilated cardiomyopathy and conduction-system disease. N Engl J Med 1999;341:1715–24.
[14] Quarta G, Syrris P, Ashworth M, Jenkins S, Zuborne Alapi K, Morgan J, Muir A, Pantazis A, McKenna WJ, Elliott PM. Mutations in the Lamin A/C gene mimic arrhythmogenic right ventricular cardiomyopathy. Eur Heart J 2012;33:1128–36.
[15] Valtuille L, Paterson I, Kim DH, Mullen J, Sergi C, Oudit GY. A case of lamin A/C mutation cardiomyopathy with overlap features of ARVC: a critical role of genetic testing. Int J Cardiol 2013;168:4325–7.
[16] Marcus FI, McKenna WJ, Sherrill D, Basso C, Bauce B, Bluemke DA, Calkins H, Corrado D, Cox MG, Daubert JP, Fontaine G, Gear K, Hauer R, Nava A, Picard MH, et al. Diagnosis of arrhythmogenic right ventricular cardiomyopathy/dysplasia: proposed modification of the task force criteria. Circulation 2010;121:1533–41.
[17] Kircher M, Witten DM, Jain P, O'Roak BJ, Cooper GM, Shendure J. A general framework for estimating the relative pathogenicity of human genetic variants. Nat Genet 2014;46:310–5.
[18] Sako H, Hadama T, Miyamoto S, Anai H, Wada T, Takahashi N, Yoshimatsu H. Successful surgical treatment of heart failure and ventricular tachycardia in a patient with arrhythmogenic right ventricular dysplasia with cardiomyopathy. Circ J 2005;69:996–9.
[19] Marcus FI, Fontaine GH, Guiraudon G, Frank R, Laurenceau JL, Malergue C, Grosgogeat Y. Right ventricular dysplasia: a report of 24 adult cases. Circulation 1982;65:384–98.
[20] McKenna WJ, Thiene G, Nava A, Fontaliran F, Blomstrom-Lundqvist C, Fontaine G, Camerini F. Diagnosis of arrhythmogenic right ventricular dysplasia/cardiomyopathy. Task Force of the Working Group Myocardial and Pericardial Disease of the European Society of Cardiology and of the Scientific Council on Cardiomyopathies of the International Society and Federation of Cardiology. Br Heart J 1994;71:215–8.
[21] Beffagna G, Occhi G, Nava A, Vitiello L, Ditadi A, Basso C, Bauce B, Carraro G, Thiene G, Towbin JA, Danieli GA, Rampazzo A. Regulatory mutations in transforming growth factor-beta3 gene cause arrhythmogenic right ventricular cardiomyopathy type 1. Cardiovasc Res 2005;65:366–73.
[22] van Tintelen JP, Van Gelder IC, Asimaki A, Suurmeijer AJ, Wiesfeld AC, Jongbloed JD, van den Wijngaard A, Kuks JB, van Spaendonck-Zwarts KY, Notermans N, Boven L, van den Heuvel F, Veenstra-Knol HE, Saffitz JE, Hofstra RM, et al. Severe cardiac phenotype with right ventricular predominance in a large cohort of patients with a single missense mutation in the DES gene. Heart Rhythm 2009;6:1574–83.
[23] Merner ND, Hodgkinson KA, Haywood AF, Connors S, French VM, Drenckhahn JD, Kupprion C, Ramadanova K, Thierfelder L, McKenna W, Gallagher B, Morris-Larkin L, Bassett AS, Parfrey PS, Young TL. Arrhythmogenic right ventricular cardiomyopathy type 5 is a fully penetrant, lethal arrhythmic disorder caused by a missense mutation in the TMEM43 gene. Am J Hum Genet 2008;82:809–21.
[24] van der Zwaag PA, van Rijsingen IA, Asimaki A, Jongbloed JD, van Veldhuisen DJ, Wiesfeld AC, Cox MG, van Lochem LT, de Boer RA, Hofstra RM, Christiaans I, van Spaendonck-Zwarts KY, Lekanne dit Deprez RH, Judge DP, Calkins H, et al. Phospholamban R14del mutation in patients diagnosed with dilated cardiomyopathy or arrhythmogenic right ventricular cardiomyopathy: evidence supporting the concept of arrhythmogenic cardiomyopathy. Eur J Heart Fail 2012;14:1199–207.
[25] Taylor M, Graw S, Sinagra G, Barnes C, Slavov D, Brun F, Pinamonti B, Salcedo EE, Sauer W, Pyxaras S, Anderson B, Simon B, Bogomolovas J, Labeit S, Granzier H, et al. Genetic variation in titin in arrhythmogenic right ventricular cardiomyopathy–overlap syndromes. Circulation 2011;124:876–85.
[26] Bertrand AT, Chikhaoui K, Yaou RB, Bonne G. Clinical and genetic heterogeneity in laminopathies. Biochem Soc Trans 2011;39:1687–92.
[27] Arimura T, Onoue K, Takahashi-Tanaka Y, Ishikawa T, Kuwahara M, Setou M, Shigenobu S, Yamaguchi K, Bertrand AT, Machida N, Takayama K, Fukusato M, Tanaka R, Somekawa S, Nakano T, et al. Nuclear accumulation of androgen receptor in gender difference of dilated cardiomyopathy due to lamin A/C mutations. Cardiovasc Res 2013;99:382–94.

Please cite this article in press as: Kato K, et al. *LMNA* cardiomyopathy detected in Japanese arrhythmogenic right ventricular cardiomyopathy cohort. J Cardiol (2015), http://dx.doi.org/10.1016/j.jjcc.2015.10.013

Circulation Journal
Official Journal of the Japanese Circulation Society
http://www.j-circ.or.jp

ORIGINAL ARTICLE
Molecular Cardiology

Molecular Mechanisms Underlying Urate-Induced Enhancement of Kv1.5 Channel Expression in HL-1 Atrial Myocytes

Nani Maharani, MD; Ya Kuang Ting, MD, PhD; Jidong Cheng, MD, PhD; Akira Hasegawa, PhD; Yasutaka Kurata, MD, PhD; Peili Li, MD, PhD; Yuji Nakayama, PhD; Haruaki Ninomiya, MD, PhD; Nobuhito Ikeda, PhD; Kumi Morikawa, PhD; Kazuhiro Yamamoto, MD, PhD; Naomasa Makita, MD, PhD; Takeshi Yamashita, MD, PhD; Yasuaki Shirayoshi, PhD; Ichiro Hisatome, MD, PhD

Background: Hyperuricemia induces endothelial dysfunction, oxidative stress and inflammation, increasing cardiovascular morbidities. It also raises the incidence of atrial fibrillation; however, underlying mechanisms are unknown.

Methods and Results: The effects of urate on expression of Kv1.5 in cultured mouse atrial myocytes (HL-1 cells) using reverse transcriptase-PCR, immunoblots, flow cytometry and patch-clamp experiments were studied. Treatment with urate at 7 mg/dl for 24 h increased the Kv1.5 protein level, enhanced ultra-rapid delayed-rectifier K^+ channel currents and shortened action potential duration in HL-1 cells. HL-1 cells expressed the influx uric acid transporter (UAT), URATv1, and the efflux UATs, ABCG2 and MRP4. An inhibitor against URATv1, benzbromarone, abolished the urate effects, whereas an inhibitor against ABCG2, KO143, augmented them. Flow cytometry showed that urate induced an increase in reactive oxygen species, which was abolished by the antioxidant, N-acetylcysteine (NAC), and the NADPH-oxidase inhibitor, apocynin. Both NAC and apocynin abolished the enhancing effects of urate on Kv1.5 expression. A urate-induced increase in the Kv1.5 proteins was accompanied by phosphorylation of extracellular signal-regulated kinase (ERK), and was abolished by an ERK inhibitor, PD98059. NAC abolished phosphorylation of ERK by urate.

Conclusions: Intracellular urate taken up by UATs enhanced Kv1.5 protein expression and function in HL-1 atrial myocytes, which could be attributable to ERK phosphorylation and oxidative stress derived from nicotinamide adenine dinucleotide phosphate (NADPH)-oxidase. (*Circ J* 2015; **79:** 2659–2668)

Key Words: Atrial fibrillation; ERK; Kv1.5; Oxidative stress; Urate

Compared to other mammals whose serum urate levels are 0.5–1 mg/dl or less, humans have a higher serum urate level due to loss of uricase activity.[1] Hyperuricemia, defined as a condition with the serum urate level exceeding 6.8 mg/dl, is a risk factor for gout, kidney stone and renal failure.[2,3] Recently, the guideline in Japan has indicated that hyperuricemia is defined as the serum urate level of more than 7 mg/dl.[4] It is caused by an imbalance between urate synthesis and its renal excretion; the predominant cause is reduced excretion due to altered expression of uric acid transporters (UATs) in the kidney. UATs in renal proximal tubular cells play a pivotal role in the regulation of serum urate levels.[5,6]

Hyperuricemia has been reported to be associated with various kinds of diseases such as hypertension, metabolic syn-

Received April 13, 2015; revised manuscript received September 7, 2015; accepted September 13, 2015; released online October 16, 2015 Time for primary review: 18 days

Division of Regenerative Medicine and Therapeutics, Department of Genetic Medicine and Regenerative Therapeutics, Institute of Regenerative Medicine and Biofunction, Tottori University Graduate School of Medical Science, Yonago (N. Maharani, Y.K.T., A.H., P.L., N.I., K.M., Y.S., I.H.), Japan; Department of Pharmacology and Therapeutics, Faculty of Medicine Diponegoro University, Semarang (N. Maharani), Indonesia; Department of Internal Medicine, The First Affiliated Hospital of Shantou University Medical College, Guangdong (J.C.), China; Department of Physiology, Kanazawa Medical University, Ishikawa (Y.K.); Division of Functional Genomics, Research Center for Bioscience and Technology (Y.N.), Department of Biological Regulation (H.N.), Department of Molecular Medicine and Therapeutics (K.Y.), Tottori University Faculty of Medicine, Yonago; Department of Molecular Physiology, Nagasaki University Graduate School of Biomedical Science, Nagasaki (N. Makita); and The Cardiovascular Institute, Tokyo (T.Y.), Japan
K.M.'s present affiliation: Center for Promoting Next-Generation Highly Advanced Medicine, Tottori University Hospital, Tottori, Japan
Mailing address: Nani Maharani, MD, Division of Regenerative Medicine and Therapeutics, Institute of Regenerative Medicine and Biofunction, Tottori University Graduate School of Medical Sciences, 86 Nishi-chou, Yonago 683-8503, Japan. E-mail: maharani.nani@gmail.com
ISSN-1346-9843 doi:10.1253/circj.CJ-15-0416

Table 1. Sequences of Mouse Uric Acid Tranporters' cDNA Primers

No.	Transcript	Reference sequence	Product (bp)	Forward primer Sequence 5'–3'	Reverse primer Sequence 5'–3'
1	URAT1	NM_009203.3	431	CAGTCCATCTTCCTGGCTGG	AGCTTGCCCACCGTGATGAG
2	URATv1	NM_001102414.1	576	GAGGAGGACAAAGAAATGGTCC	ATCACTCCGAACAGGTATGGC
3	ABCG2	NM_011920.3	496	CCTACAACAACCCTGCGGAT	ACTACGAACAGCTCCACAGC
4	NPT1	NM_009198.3	665	GATGTCCTTGCTCCTCCCAC	TGGTGAAGAGTTTCCGGACG
5	NPT4	NM_001164743.1	527	TCACACTGATGGCGCAGAAT	ACTAATGATGCCGCCCACAA
6	OAT1	NM_008766.3	331	ACCTTGTGTGCTCTCATCGG	AACTGGCCCAAGCTGTAGAC
7	OAT3	NM_031194.5	308	CTTCCGATTCCTGTGTGGCT	TAGCCACACGTTGGAGTGTC
8	MRP4	NM_001163676.1	426	CGTTAATTGAGGCACTCCGGT	GGTAGGAGCTGCCCAGAATC
9	MCT9	NM_025807.3	330	CCTTCCTAAAAGCCTCGCCA	CCCAAAAGAAGCTTGCCCAC

ABCG2, ATP-binding cassettes subfamily G second member 2 (also known as the human breast cancer resistance protein [BRCP]); bp, base pairs; MCT, monocarboxylate transporter; MRP, multidrug resistance protein; NPT, Na^+/phosphate cotransporter; OAT, organic anion transporter; URAT, urate transporter.

dromes, diabetes mellitus, as well as chronic kidney disease.[5,7–9] It increases oxidative stress, endothelial dysfunction and inflammation, thereby increasing cardiovascular morbidity and mortality.[7,8] Two possible mechanisms have been proposed for hyperuricemia-related cardiovascular dysfunction: (1) xanthine oxidase causes oxidative stress; and (2) urate induces vascular smooth muscle cell proliferation, decreases nitric oxide production and activates the renin-angiotensin system.[10–13] UATs (eg, URAT1) are expressed not only in renal tubular cells, but also in vascular smooth muscle cells, endothelial cells, adipocytes and pancreatic β-cells.[5,14–16] Thus, intracellular accumulation of urate via activation of UATs could cause systemic cell damage through several signaling pathways.[13,15,17]

Several clinical studies have reported a strong association between hyperuricemia and the incidence of atrial fibrillation (AF) in patients with hypertension,[18] type 2 diabetes mellitus,[19] and/or cardiovascular diseases[20] such as chronic heart failure,[21] ischemic heart failure,[22] and cardiac events.[23] Another cohort study reported that hyperuricemia was associated with the development of AF, indicating that the serum urate level is a predictor for comorbidity with AF.[24] High levels of serum urate correlated with not only recurrence of paroxysmal AF after catheter ablation,[25] but also permanent AF,[26] and increased risk of left atrial thrombus as well as thromboembolic risk on transesophageal echocardiography in patients with non-valvular AF.[27,28] Suzuki et al recently reported that serum urate could be a marker or an independent risk factor for AF in patients with cardiovascular diseases.[20] These reports indicate that the measurement of the serum urate level could be useful in predictions of the onset and prognosis in AF patients,[23] and the control of the serum urate level might be a therapeutic approach for AF. Despite these correlations, however, the mechanisms underlying the occurrence of AF in hyperuricemia patients remains unknown.

AF is triggered by ectopic activity in the atrium or pulmonary vein and is sustained by reentry that is characterized by shortening of the effective refractory period (ERP), unidirectional conduction block and slow conduction.[29] Electrical properties of atrial myocytes in AF depend on electrical remodeling, namely, altered expressions of atrial ion channels.[30] Shortening of the atrial action potential duration (APD) shortens ERP, which plays an important role in the initiation and sustainment of AF.[30] Both rate and rhythm control are essential in AF management, however, their application must be considered wisely due to serious adverse effects and limited long-term efficacy.[31]

Kv1.5 channels (voltage-gated potassium channel, shaker-related subfamily, member 5), encoded by the *KCNA5* gene, confer the ultra-rapid delayed-rectifier potassium channel currents (I_{Kur}) that strongly influence APD. It is more abundantly expressed in the human atrium than in the ventricle.[32] The increases in mRNA and protein levels of Kv1.5 channels contribute to the shortening of atrial APD, causing electrical remodeling with atrial APD shortening in AF; therefore, inhibition of Kv1.5 channel expression may be one of the therapeutic approaches for AF.[33–35]

HL-1 cells are cardiac muscle cells derived from the AT-1 mouse atrial cardiomyocyte tumor lineage. They are able to contract spontaneously, propagate with an apparently unlimited lifespan, and express the ion channels required for generating action potentials.[36,37] They have been used for studying Kv1.5 channels, as reported in several publications.[37,38]

Taken together, we hypothesized that urate could enhance the expression of Kv1.5 in atrial myocytes. To verify this hypothesis, we studied the effects of urate on the expression and function of Kv1.5 channels using HL-1 cells, and explored subcellular mechanisms underlying the hyperuricemia-induced increase in AF incidence and alteration of Kv1.5 channels to facilitate AF occurrence.

Methods

Cell Culture

HL-1 cells were cultured in Claycomb medium supplemented with 10% Fetal bovine serum, 1% norepinephrine, 1% penicillin-streptomycin, and 1% L-glutamin, on dishes coated with 0.02% gelatin-fibronectin in an incubator at 37°C with 5% CO_2, before being subjected to the assays.

Reagents

Urate (uric acid sodium salt) (Sigma Aldrich, St. Louis, MO, USA) was dissolved in 10 mmol/L NaOH. It was administered to cells at 60–70% confluence at the final concentration of 7 mg/dl. We also used the influx UAT (URATv1) inhibitor, benzbromarone, and efflux UAT (ABCG2) inhibitor, KO143 (Sigma Aldrich), antioxidant N-acetylcysteine (NAC) (Sigma Aldrich), NADPH-oxidase inhibitor, apocynin (Abcam Biochemicals), and an extracellular signal-regulated kinase (ERK) inhibitor, PD98059 (Sigma Aldrich).

mRNA Extraction and Reverse Transcriptase-PCR

Total RNA was extracted from HL-1 cells and mouse kidney using a RNeasy kit (Qiagen). cDNA was synthesized using PrimeScript with gDNA eraser (Takara Bio Inc, Kusatsu,

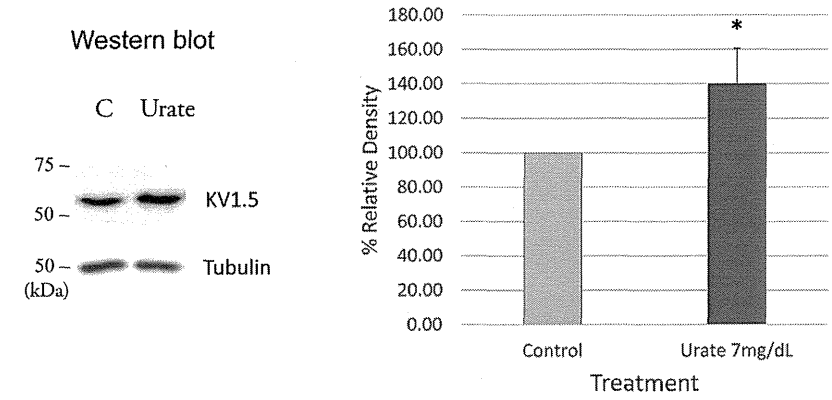

Figure 1. Effects of urate on Kv1.5 protein levels in HL-1 cells. Protein expressions were analyzed by Western blotting using anti-Kv1.5 and anti-α-tubulin as an internal control. Representative Western blots (**Left**) and averaged densities of Kv1.5 proteins normalized to those of α-tubulin (**Right**) are shown. HL-1 cells were treated with urate at 7 mg/dl or urate's solvent (10 mmol/L NaOH) as a control for 24 h. The relative density of Kv1.5 proteins in the urate-treated group is shown as a percentage to the control value (n=14; *P<0.05).

Japan) according to the manufacturer's protocol. PCR primers are listed in **Table 1**.

Western Blot Analysis

Cells were collected in lysis buffer containing 0.01 M phosphate buffered saline (PBS), 1% nonidet P-40 (w/w), 0.5% sodium deoxycholate (w/v), 0.1% sodium dodecyl sulphate (w/v), 10 μg/ml aprotinin, 10 μg/ml leupeptine, 10 μg/ml pepstatin and 1 mmol/L phenylmethylsulfonyl fluoride, and were lysed by repeat pipetting. Insoluble materials were removed by centrifugation, and the protein concentration of the supernatant was determined by using the Bradford Protein Assay method. An aliquot of 10–15 μg protein was subjected to sodium dodecylsulfate poly-acrylamide gel electrophoresis and electrotransferred to a polyvinylidene fluoride membrane. After being blocked with 5% skim milk, membranes were probed with primary antibodies against Kv1.5 (1:400; Alomone Labs, Jerussalem, Israel), α-tubulin (1:5,000; Abcam, Tokyo, Japan), phosphorylated ERK (1:500; Cell-signaling Technology) or total ERK (1:1,000; Cell-signaling Technology). The secondary antibodies were either anti-rabbit IgG or anti-mouse IgG (1:3,000); both are horseradish-peroxidase-linked (GE-Healthcare Limited, Buckinghamshire, UK). The blots were developed using the enhanced chemiluminescence (ECL) system (Amersham Bioscience, Piscataway, NJ, USA). The band intensities were quantified using Image J version 1.42q software (NIH, Bethesda, MD, USA).

Assay of Reactive Oxygen Species (ROS) Level

HL-1 cells were treated with urate (7 mg/dl) alone, urate (7 mg/dl) with either NAC (10 mmol/L) or apocynin (1 mmol/L), or the solvent NaOH (10 mmol/L) as a control, washed with PBS, and incubated in the presence of 20 μmol/L 2',7'-Dichlorofluorescin diacetate (DCFH-DA) (Sigma Aldrich) for 30 min. Cells were then washed with PBS, trypsinized, resuspended in fluorescence-activated cell sorting (FACS) buffer, and analyzed by BD FACSAria™ flowcytometry (BD Bioscience, San Jose, CA, USA).

Electrophysiological Recordings

After treatment with urate, Kv1.5 channel currents corresponding to I_{Kur} were measured. Outward membrane currents were elicited every 6 s by 300-ms test pulses ranging from –60 to +80 mV (in 10 mV increments) with a holding potential (HP) of –60 mV. A specific inhibitor of Kv1.5 channel currents, 4-aminopyridine (4-AP), at a dose of 100 μmol/L was used to isolate I_{Kur}. To eliminate the contamination by another outward current, rapidly activating delayed rectifier potassium channel current (I_{Kr}), the outward currents were recorded in the presence of 5 μmol/L E4031, which blocked I_{Kr} almost completely. Thus, the currents measured here were 4-AP-sensitive, E4031-insensitive currents. The extracellular solution contained (in mmol/L) 140 NaCl, 4 KCl, 1.8 $CaCl_2$, 0.53 $MgCl_2$, 0.33 NaH_2PO_4, 5.5 glucose, and 5 HEPES, with the pH adjusted to 7.4 by NaOH. The internal pipette solution contained (in mmol/L) 100 K-aspartate, 20 KCl, 1 $CaCl_2$, 5 Mg-ATP, 5 EGTA, 5 HEPES, and 5 creatine phosphate dipotassium (pH 7.2 with KOH). Patch pipettes had a resistance of 5–10 MΩ when filled with the pipette solution. Series resistance (R_s) was determined by fitting a single exponential function to the capacitive current decay to estimate its time constant and membrane capacitance. After the R_s compensation of 50–60%, the voltage errors arising from R_s were estimated to be less than 5 mV. The membrane potential was not corrected for the liquid junction potential, which was estimated to be <10 mV. Currents were recorded with an Axopatch-200B amplifier (Axon Instruments, Union City, CA, USA). The capacity-corrected data were digitally filtered at 2 kHz, then analyzed using pCLAMP9 software on the computer. Action potentials were measured in current-clamp mode, elicited at a rate of 0.5 Hz by 5-ms square current pulses of 1 nA, and sampled at 20 kHz. All currents and AP measurements were conducted at 37°C.

Statistical Analysis

The data were presented as mean±SD, and the graphs were built using Excel 2013 for Windows. Data were checked for its distribution before further analysis. To analyze the difference between the 2 groups, the Student's unpaired t-test was

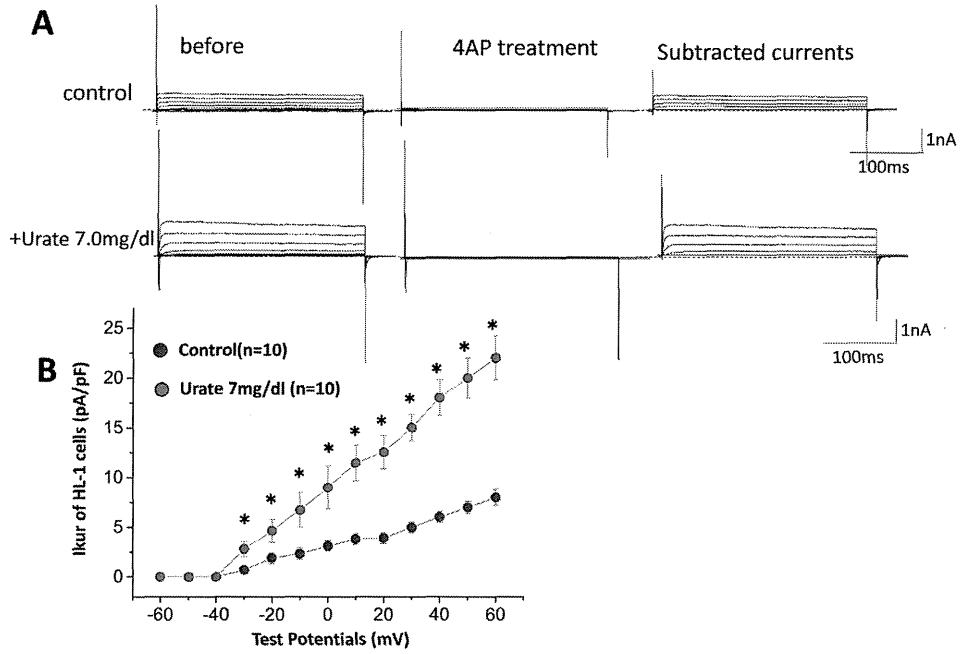

Figure 2. Effects of urate on the Kv1.5 channel current, the ultra-rapid delayed rectifier potassium channel currents (I_{Kur}). (**A**) Patch clamp records of outward membrane currents elicited before (**Left**) and during (**Middle**) administration of 4-aminopyridine (4-AP; 100 μmol/L) in HL-1 cells treated with or without urate at 7 mg/dl. 4-AP-sensitive currents were determined by subtracting the current in the presence of 4-AP from that in the absence of the agent (**Right**). All current measurements were conducted in the presence of 5 μmol/L E4031, which eliminates rapid delayed-rectifier potassium channel currents (I_{Kr}). (**B**) Voltage-dependent activation of 4AP-sensitive currents recorded from the urate-treated (red circles) and control (blue circles) cells. Peak amplitudes of the outward currents were determined and plotted as functions of the test potentials. The currents from the urate-treated cells were significantly larger than those from the urate-untreated cells (*P<0.05).

used. Analysis of variance (ANOVA) followed by Fisher's Least Significant Difference (LSD) post-hoc test was used to assess the difference between multiple groups. A P value of <0.05 was considered significant. All of the statistical analyses were performed by using OriginPro 9.1.0 (OriginLab Corporation, Northampton, MA, USA).

Results

Urate Increased Kv1.5 Protein Levels and Enhanced I_{Kur}

Figure 1 shows the representative Western blot of Kv1.5 proteins expressed by HL-1 cells treated for 24 h with or without urate (7 mg/dl). The summarized data on the density of Kv1.5 proteins normalized to α-tubulin density confirmed that urate significantly increased the protein level of Kv1.5. To examine whether urate increases the activity of Kv1.5 channels on the cell surface, we measured I_{Kur} through Kv1.5 channels. **Figure 2A** shows original current traces of 4-AP-sensitive I_{Kur} in HL-1 cells treated with or without urate (7 mg/dl). Depolarizing test pulses elicited outward currents, which were almost completely blocked by 4-AP at 100 μmol/L. As HL-1 cells were known to express another component of outward currents, I_{Kr}, we eliminated I_{Kr} contamination using the I_{Kr} inhibitor, E4031. Treatment with urate for 24 h increased the amplitude of I_{Kur} elicited by the depolarizing pulses from a HP of –60 mV. Urate did not influence the capacitive currents (35±3.2 pF in control, 36.7±3.0 pF with urate). Summary data of the voltage-dependent activation of I_{Kur} in HL-1 cells in the absence and presence of urate indicate that urate significantly augmented I_{Kur} in a potential range from –30 to +60 mV without affecting the threshold potential (**Figure 2B**). Urate did not affect the L-type calcium channel currents or protein level, as shown in **Figures S1** and **S2**.

Figure 3 shows the representative action potentials recorded from HL-1 cells treated with (black and blue) or without urate (red and green), and averaged APDs at 50% repolarization (APD_{50}) and 90% repolarization (APD_{90}). Urate significantly shortened APD_{50} (32.83±6.51 ms in control, 17.74±5.85 ms with urate) and APD_{90} (113.18±18.51 ms in control, 53.28±23.29 ms with urate) without changes in resting membrane potentials (–69.38±2.85 mV in control; –69.60±1.77 mV with urate). The details on action potential parameters are presented in **Table 2**. To ensure that the changes in APDs were specifically caused by the increase of I_{Kur}, we also compared APDs in the control and urate groups in the absence and presence of 4-AP. The results showed that after addition of 4-AP, the APDs in urate-treated cells were significantly prolonged, but shorter than those in the control group.

Inhibition of UATs Influenced a Urate-Induced Increase in Kv1.5 Channel Proteins in HL-1 Cells

We evaluated the mRNA expression of 9 UATs in HL-1 cells

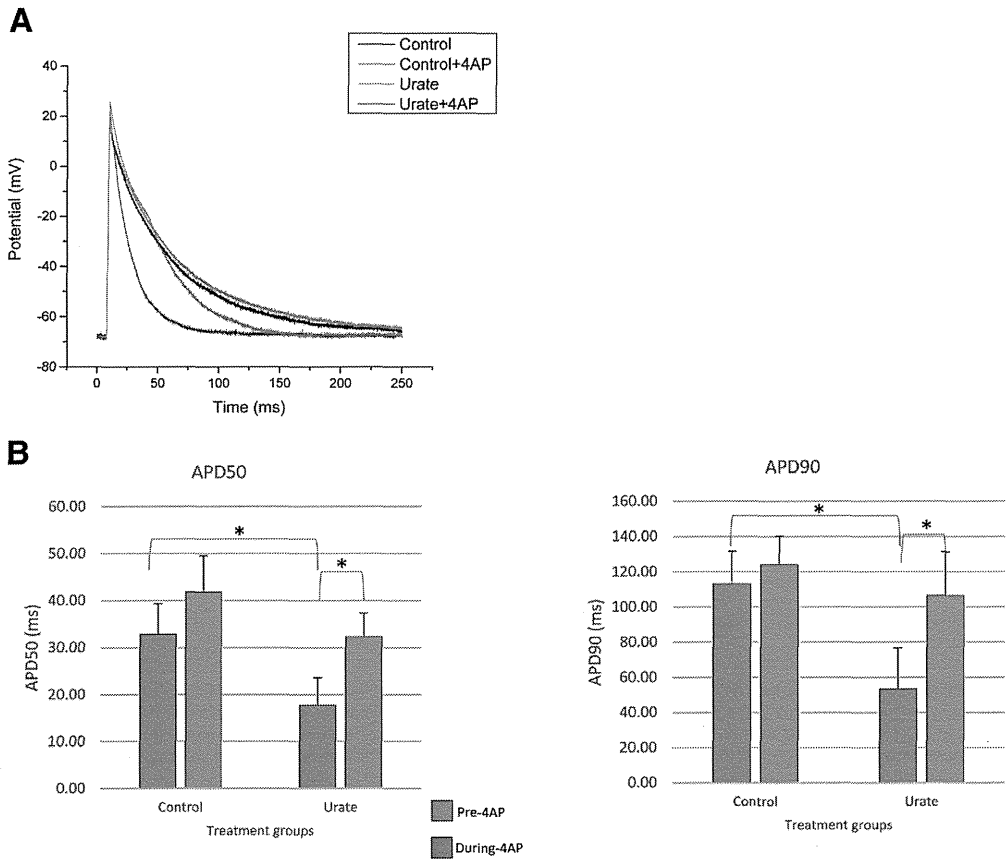

Figure 3. Effects of urate on action potentials of HL-I cells. (**A**) Action potentials recorded from HL-1 cells treated with (blue and pink) or without (black and red) urate at 7 mg/dl before and during application of 4-aminopyridine (4-AP). (**B**) Action potential durations at 50% repolarization (APD_{50}) and 90% repolarization (APD_{90}) measured for the control and urate-treated cells. Both APD_{50} and APD_{90} values were significantly shorter in the urate-treated cells than in control cells (n=10; *P<0.05).

Table 2. Action Potential Parameters

No.	Treatment group	Resting membrane potential (mV)	AP amplitude (mV)	Overshoot (mV)	APD_{50} (ms)	APD_{90} (ms)
1	Control	−69.38±2.85	90.73±6.69	21.35±7.03	32.83±6.51	113.18±18.51
2	Urate	−69.60±1.77	87.45±5.21	17.85±5.20	17.74±5.85	53.28±23.39

APD_{50}, action potential durations at 50% repolarization; APD_{90}, action potential durations at 90% repolarization.

using RT-PCR (**Figure 4A**), which detected the expressions of an influx transporter (URATv1) and two efflux transporters (ABCG2 and MRP4). All of these expressed UATs were also expressed in human embryonic stem cell-derived cardiomyocytes (**Figure S3**).

To test how the expressed UATs could be involved in the urate-induced enhancement of Kv1.5 protein expression, we examined the effects of UATs inhibitors on the Kv1.5 protein expression in HL-1 cells. **Figure 4B** shows the representative Western blots of expressed Kv1.5 proteins after a 24-h treatment with or without urate. Pretreatment with benzbromarone (20μmol/L), an inhibitor of the influx transporter, URATv1, abolished the urate-induced increases in Kv1.5 protein expression. **Figure 4C** shows the representative Western blots of Kv1.5 proteins after a 24-h treatment with or without urate in the absence and presence of KO143 (100 nmol/L), an inhibitor of the efflux urate transporter, ABCG2. KO143 (100 nmol/L) enhanced the urate-induced increase in Kv1.5 protein expression. Either benzbromarone or KO143 alone did not affect the Kv1.5 expression (data not shown).

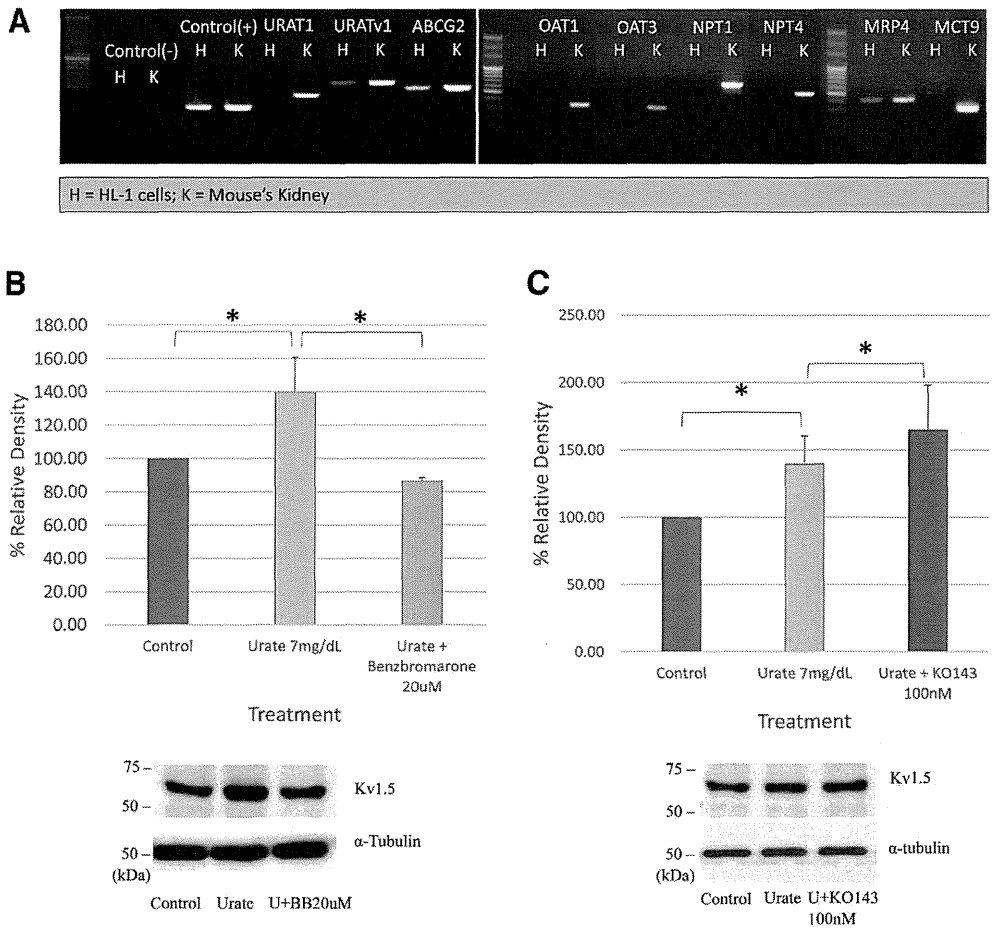

Figure 4. Expression of uric acid transporters (UATs) and their roles in urate-induced Kv1.5 upregulation in HL-1 cells. (**A**) mRNA expressions of UATs in HL-1 cells determined by polymerase chain reaction (PCR) analyses. Data for HL-1 cells' cDNA (H) and mouse kidney's cDNA as a control (K) are shown in pairs. HL-1 cells expressed URATv1, ABCG2 and MRP4. Control (–) indicates a control for gDNA contamination during reverse-transcriptase reaction, of which the reverse-transcriptase enzyme was not added to the reaction. Control (+) means a control for the reverse-transcription process, indicating that cDNAs could be well synthesized. During amplification, glyceraldehyde 3-phosphate dehydrogenase (GAPDH) primers were added to both Controls. (**B**) Effect of benzbromarone on the expression of Kv1.5 proteins. HL-1 cell cultures were assigned to 3 groups, and treated with 10 mmol/L of NaOH as a control, 7 mg/dl urate alone, or 7 mg/dl urate with 20 μmol/L benzbromarone. Protein lysates were taken after 24 h. Representative Western blots (**Lower**) and the averaged density of Kv1.5 proteins normalized to that of α-tubulin (**Upper**) are shown. The averaged density data shown as percentages to the control values revealed a significant increase of Kv1.5 expression in the group administered urate alone, and a reduction of the urate effect in the presence of 20 μmol/L benzbromarone (n=3; *P<0.05). (**C**) Effect of KO143 on the expression of Kv1.5 proteins. HL-1 cell cultures were assigned to 3 groups, treated with 10 mmol/L NaOH as a control, 7 mg/dl urate alone, or 7 mg/dl urate with 100 nmol/L KO143. Protein lysates were taken after 24 h. Representative Western blots (**Lower**) and the averaged density of Kv1.5 normalized to that of α-tubulin (**Upper**) are shown. The averaged density data demonstrate an increased Kv1.5 expression in the group treated with urate alone, and a further increase of Kv1.5 expression in the presence of KO143 (n=4; *P<0.05).

Oxidative Stress Is Involved in Urate-Induced Upregulation of Kv1.5 Channel Proteins

We also examined whether oxidative stress was involved in the urate-induced enhancement of Kv1.5 expression. Treatment with urate increased ROS by approximately 30%, and this effect was cancelled by simultaneous treatment with an antioxidant, NAC (**Figure 5A Left**). **Figure 5B (Left)** shows the representative Western blots of Kv1.5 proteins after 24-h treatment with or without urate in the absence and presence of NAC. Treatment with NAC (10 mmol/L) for 1 h prior to urate exposure abolished the enhancing effect of urate on Kv1.5 protein expression, while NAC alone did not affect the Kv1.5 expression (data not shown).

As ROS generation induced by urate has been reported to involve nicotinamide adenine dinucleotide phosphate (NADPH)-oxidase, we tested the effects of a NADPH-oxidase

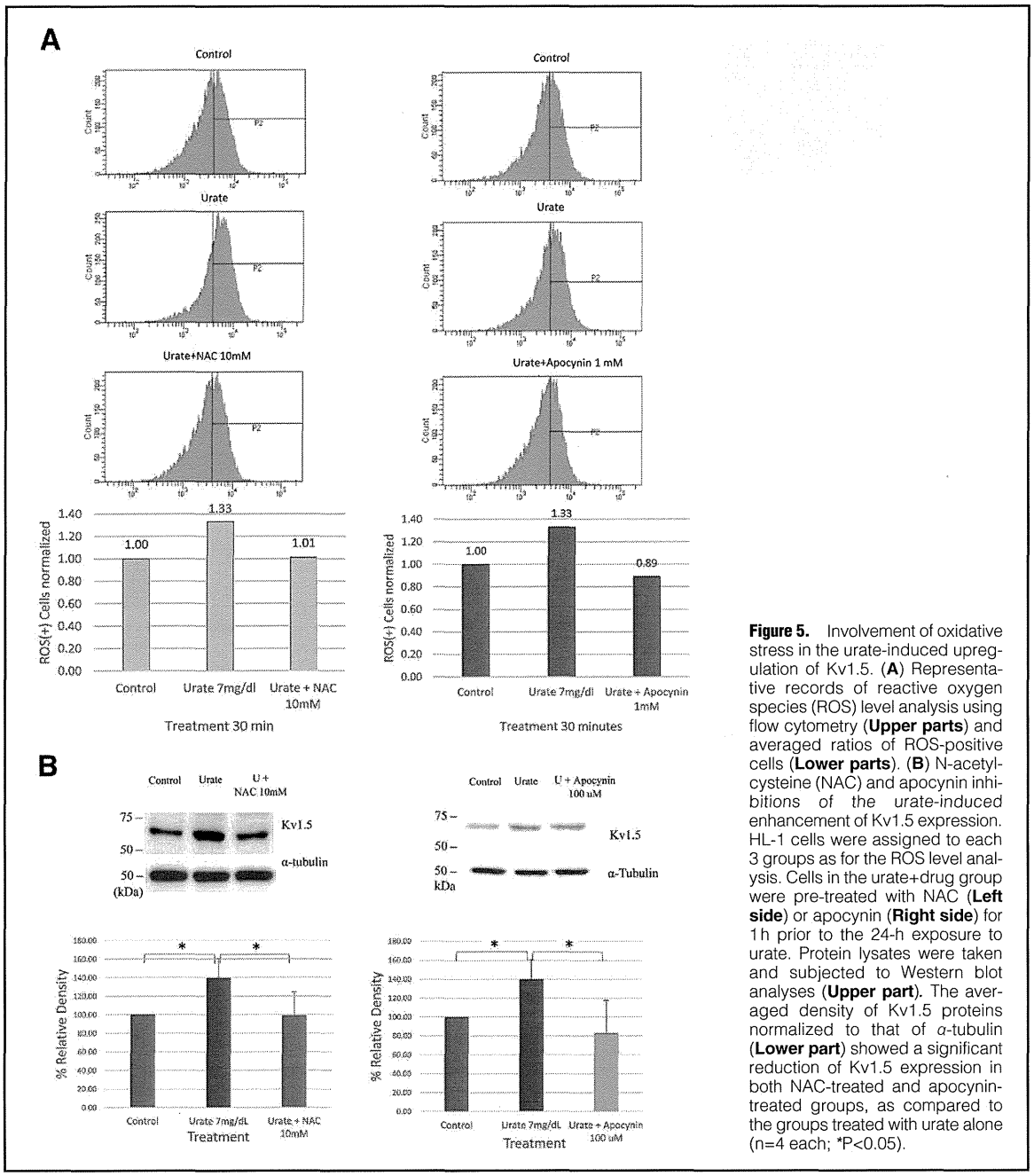

Figure 5. Involvement of oxidative stress in the urate-induced upregulation of Kv1.5. (**A**) Representative records of reactive oxygen species (ROS) level analysis using flow cytometry (**Upper parts**) and averaged ratios of ROS-positive cells (**Lower parts**). (**B**) N-acetylcysteine (NAC) and apocynin inhibitions of the urate-induced enhancement of Kv1.5 expression. HL-1 cells were assigned to each 3 groups as for the ROS level analysis. Cells in the urate+drug group were pre-treated with NAC (**Left side**) or apocynin (**Right side**) for 1 h prior to the 24-h exposure to urate. Protein lysates were taken and subjected to Western blot analyses (**Upper part**). The averaged density of Kv1.5 proteins normalized to that of α-tubulin (**Lower part**) showed a significant reduction of Kv1.5 expression in both NAC-treated and apocynin-treated groups, as compared to the groups treated with urate alone (n=4 each; *P<0.05).

inhibitor, apocynin. **Figure 5A (Right)** shows the effects of apocynin on ROS productions in the presence of urate. Flow cytometry confirmed the increase of ROS in the urate-treated group, and that apocynin at 1 mmol/L reduced ROS to the control level. **Figure 5B (Right)** shows the representative Western blots of Kv1.5 proteins after 24-h treatment with or without urate. Treatment with apocynin on urate-treated cells abolished the urate-induced enhancement of Kv1.5 expression. Apocynin alone did not affect Kv1.5 expression (data not shown). Each of the flow cytometry experiments was confirmed by another experiment.

ERK Pathway Is Involved in Urate-Induced Kv1.5 Upregulation

We further examined an involvement of the ERK pathway, the downstream signaling pathway activated by oxidative stress, in the urate-induced enhancement of Kv1.5 expression. **Figure 6A** shows the representative Western blots of Kv1.5 proteins after

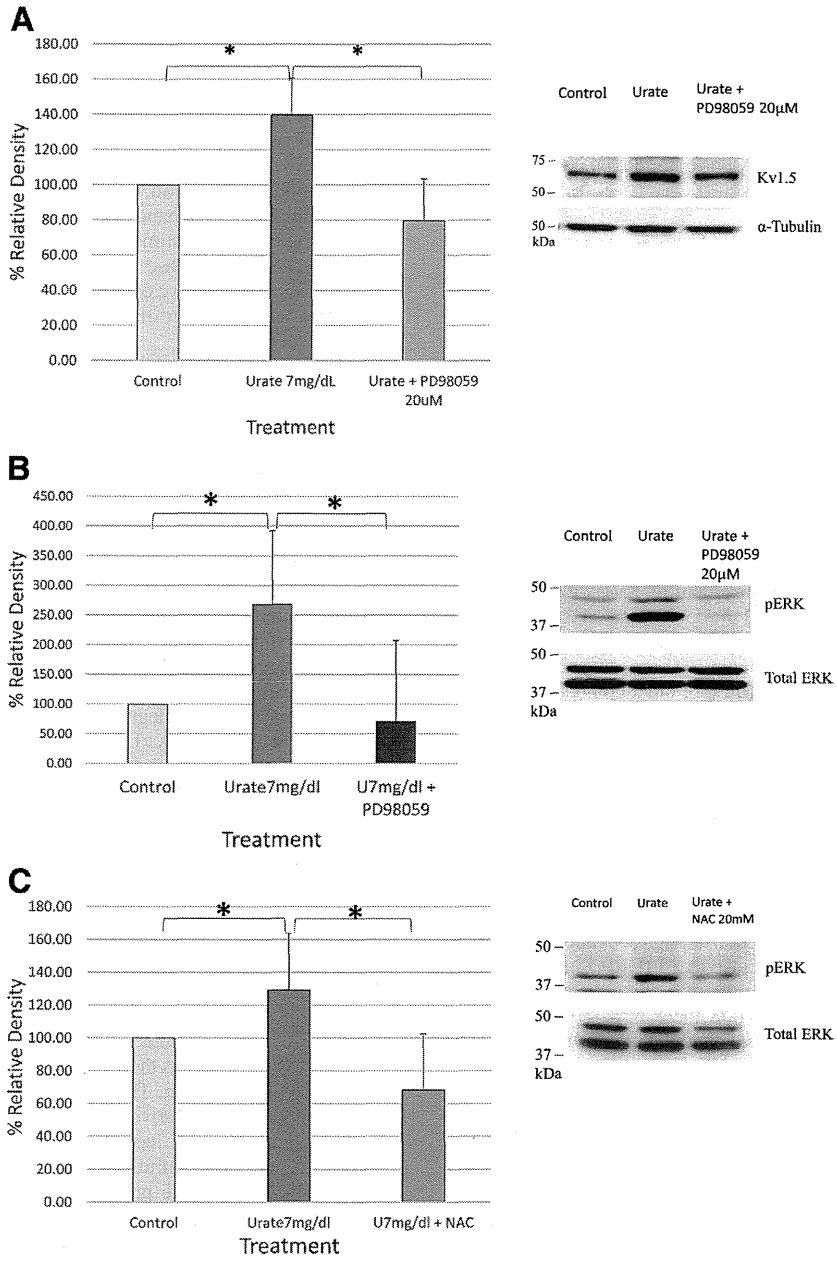

Figure 6. Involvement of the extracellular signal-regulated kinase (ERK) pathway in the urate-induced upregulation of Kv1.5. (**A**) Effect of the ERK-inhibitor, PD98059, on Kv1.5 expression. HL-1 cells were treated with NaOH at 10 mmol/L (Control), urate (7 mg/dl) alone, or urate (7 mg/dl)+PD98059 (20μmol/L) for 24 h. Protein lysates were taken, and subjected to Western blot analyses (**Right**). The averaged density of Kv1.5 proteins normalized to that of α-tubulin (**Left**) showed a significant reduction of Kv1.5 expression in the PD98059-treated group (n=3; *P<0.05). (**B**) Effect of PD98059 on phosphorylated-ERK. HL-1 cells were treated as per the Kv1.5 expression analysis described above. Western blots using an antibody against phosphorylated ERK (pERK) revealed an increase of pERK level in the urate-treated cells (right). The averaged density of pERK as a percentage to the total ERK, normalized to the density in the control group, showed significant inhibition of the urate-induced pERK increase by PD98059 (**Left**; n=3; *P<0.05). (**C**) Effect of N-acetylcysteine (NAC) on phosphorylated-ERK. HL-1 cells were treated with NaOH at 10 mmol/L (Control), urate (7 mg/dl) alone, or urate (7 mg/dl)+NAC (20 mmol/L) for 24 h. Western blots using anti-pERK antibody revealed an increase of pERK level in the urate-treated cells (**Right**). The averaged density of pERK as a percentage to the total ERK showed significant inhibition of the urate-induced-pERK-increase by NAC (**Left**; n=3; *P<0.05).

24-h treatment with or without urate in combination with an ERK inhibitor, PD98059. PD98059 (20 μmol/L) abolished the urate effect. Urate increased phosphorylated ERK (pERK) in HL-1 cells (**Figure 6B**), and PD98059 (20 μmol/L) abolished this enhancement. We finally examined effects of NAC on the level of pERK in urate-treated cells (**Figure 6C**). NAC abolished the increase of pERK caused by urate, indicating that the urate-induced enhancement of ERK phosphorylation is due to oxidative stress.

Discussion

In the present study, we investigated whether urate, a soluble form of uric acid, could alter the expression and function of Kv1.5 channels in HL-1 cells. Treatment with urate increased the protein level of Kv1.5, which was accompanied by an increase in I_{Kur} and shortening of APDs.

Kv1.5 channels, encoded by the *KCNA5* gene, confer I_{Kur}. In humans, the Kv1.5 channel is selectively expressed in atrial myocytes where it is an important contributor for action potential repolarization and controls APD.[39] Overexpression of Kv1.5 in rat cardiomyocytes shortens APD,[40] leading to the shortening of ERP, which plays an important role in the generation of reentry circuits to cause tachyarrhythmia. Yamashita et al reported that the enhancement of Kv1.5 expression by rapid pacing resulted in APD shortening and AF.[33] In the present study, the urate-induced increase in Kv1.5 expression was associated with APD shortening. This is the first study to report that intracellular elevation of urate could shorten atrial APD and ERP via enhancement of Kv1.5 channel currents. Elevation of the serum urate level has been reported to increase the incidence of AF, and a recent study has indicated that hyperuricemia is an independent risk factor of AF.[20] Our findings are consistent with these reports.

The intracellular urate level is regulated by UATs.[5,6] The intracellular accumulation of urate via activation of influx UATs could cause cellular damage through several signaling pathways. In a previous report by Kang et al, urate induced vascular smooth cell proliferation through activation of an influx UAT, voltage-driven urate transporter 1 (URATv1, also known as SLC2A9).[13] There is no report regarding the expression of UATs in human atrium, while there is a report of UATs expressed in human umbilical endothelial cells (HUVECs).[16] This report indicated that URATv1, as well as ATP-binding cassettes subfamily G second member (also known as the human breast cancer resistance protein, BRCP; ABCG2), multidrug resistance protein 4 (MRP4) and monocarboxylate transporter 9 (MCT9) were expressed in HUVECs; thus, the types of UATs in HUVECs were similar to those in HL-1 cells. We confirmed that the expressed UATs were also expressed in human embryonic stem cell-derived cardiomyocytes (**Figure S3**). Based on these data, there might be significant expressions of URATv1 and other UATs in human atrium as well. However, further experiments would be necessary to clarify whether hyperuricemia really shortens the refractory period in human atrium via the enhancement of Kv1.5 channel expression.

In the present study, HL-1 cells expressed mRNA of the influx transporter, URATv1, as well as the efflux transporters, ABCG2 and MRP4. The authentic URATv1 inhibitor benzbromarone abolished, but the ABCG2 inhibitor, KO143, enhanced the urate-induced increases of Kv1.5 proteins. These findings support our hypothesis that the intracellular accumulation of urate via UATs increases Kv1.5 proteins in HL-1 cells.

Urate-induced oxidative stress is implicated in various pathophysiological states.[10,12,15] Urate stimulates the production of oxidant in both adipocytes and vascular smooth muscle cells.[17,41] We observed an increase of ROS in urate-treated HL-1 cells. This increase was proportional to the increase of Kv1.5 proteins. Reversal of the increase by the antioxidant, NAC, confirms an involvement of oxidative stress. ROS is well-known to be generated by NADPH oxidase and urate-induced ROS production via activation of NADPH oxidase.[41] The NADPH oxidase inhibitor, apocynin, reduced the ROS level and inhibited the urate-induced enhancement of Kv1.5 expression. Chao et al reported that urate stimulated the expression of endothelin-1 and NADPH oxidase in human aortic smooth muscle cells.[41] Taken together, we conclude that urate-induced oxidative stress via activation of NADPH oxidase increased the protein level of Kv1.5.

Several studies reported involvement of the ERK 1/2 pathway as part of the downstream signaling of urate-derived ROS.[15,42] In the present study, treatment with urate increased the level of pERK, which was suppressed by pretreatment with the antioxidant, NAC. This finding is consistent with previous reports for vascular smooth muscle cells, adipocytes and pancreatic β-cells.[15,17,41] The present study demonstrates that urate enhances Kv1.5 expression through xanthine oxidase and NADPH oxidase-dependent oxidative stress, and activation of the ERK1/2 pathway.

Some limitations in this study should be considered. The Kv1.5 channel is known to have a complex regulatory mechanism, starting from its transcription, translation, and post-translational modifications affecting its glycosylation, trafficking, surface expression and degradation.[43] Our study measured only the total expressed Kv1.5; further studies are needed to clarify which part of the regulations is actually affected. The mean current increased 3-fold, while the Kv1.5 protein expression increased by only approximately 30%. This discrepancy might be caused by the involvement of other factors that we did not observe. In this study, we used the HL-1 mouse atrial myocytes cell line, of which electrophysiological and biological properties have been well characterized. However, experiments using primary cultured cardiomyocytes or in vivo studies are necessary in the future. Another limitation is that we selected only some of the commonly known UATs to be analyzed for their presence in HL-1 cells. Thus, the presence of other UATs in HL-1 cells is unknown.

In summary, urate enters the cell through UATs, and enhances Kv1.5 protein expression. This effect is exerted by NADPH oxidase-dependent oxidative stress and the ERK pathway. Because the atrium with increased Kv1.5 currents is predisposed to AF, the use of influx UAT inhibitors and antioxidants may be beneficial for the prevention of AF in patients with hyperuricemia. Confirming this finding can lead to a more comprehensive treatment of hyperuricemia, particularly for the prevention of an overexpression of K^+ channels, which may increase the risk of tachyarrhythmias, including AF.

Acknowledgments

We sincerely thank Professor William C Claycomb for the original HL-1 cells.

Source of Funding

None.

Disclosures

None.